Title
HYPERFINE-STRUCTURE MEASUREMENTS OF SOME TRANSURANIC ELEMENTS

Author
Marrus, Richard.

Publication Date
1958-11-23

UCRL 8547

UNIVERSITY OF
CALIFORNIA

Radiation
Laboratory

HYPERFINE-STRUCTURE MEASUREMENTS OF SOME TRANSURANIC ELEMENTS

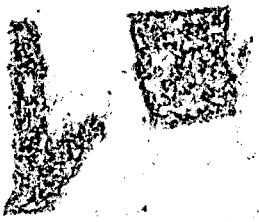

DISCLAIMER

UCRL-8547

UNIVERSITY OF CALIFORNIA

Lawrence Radiation Laboratory
Berkeley, California

Contract No. W-7405-eng-48

HYPERFINE-STRUCTURE MEASUREMENTS ON SOME TRANSURANIC ELEMENTS

Richard Marrus (thesis)

November 23, 1958

Printed for the U.S. Atomic Energy Commission

Printed in USA. Price $2.25. Available from the
Office of Technical Services
U. S. Department of Commerce
Washington 25, D. C.

Contents

ABSTRACT

Hyperfine-structure measurements have been made on four isotopes in the transuranic region by means of the atomic beam flop-in method. These measurements have yielded values of J and g_J of the low-lying electronic states of each element and values for the nuclear spin of each isotope. In addition, the hyperfine-structure splitting of Pu^{239} and the energy separations of the four observed states of Cm^{242} have been determined. The results are:

Isotope ($T_{\frac{1}{2}}$)	J	Energy Level Splitting $(cm.)^{-1}$	g_J	I	$\Delta\nu$ (Mc.)	Inferred Configuration
Pu^{239}(24,000 yrs.)	1	----------	1.4975±.0010	$\frac{1}{2}$	7.683 ±.060	$5f^6 7s^2$
Np^{238}(2.1d.)	11/2	----------	0.6551±.0006	2	----	$5f^4 6d7s^2$
Np^{239}(2.35d.)				5/2	----	
Cm^{242}(162d.)	2	550±300	2.561±.003			
	3	650±300	2.000±.003	0	----	$5f^7 6d7s^2$
	4	1000±500	1.776±.002			
	5		1.671±.003			

The spin of 1/2 measured in Pu^{239} verifies earlier measurements made by optical spectroscopy and paramagnetic resonance. From the measured value of $\Delta\nu(Pu^{239})$, it has been possible to infer a value for the nuclear magnetic moment of ±0.02 nm.

The electronic ground-state configurations have been inferred from the J and g_J values and from detailed assumptions concerning coupling of electrons in the transuranic region. The results are in agreement with the predictions of Seaborg.

The text contains a description of the theory of experiment, experimental technique, and an analysis of the results.

INTRODUCTION

This paper describes an investigation on some elements in the transuranic region as part of a general program of research on elements in the transuranic region. The purpose of this program is threefold:

1. To ascertain from direct measurement the g_J and J values of the low-lying electronic states which are accessible and to infer from these measurements the ground-state configurations and coupling schemes in the heavy-element region.

2. From direct measurement to determine the value of the spin of the nuclear ground state.

3. From measurement of the hyperfine-structure separations to try to establish the existence of dipole, quadrupole, and higher-order nuclear moments and to infer their values.

The work to be described here led to measurements carried out on the following isotopes:

$_{93}Np^{238}$

$_{93}Np^{239}$

$_{94}Pu^{239}$

$_{96}Cm^{242}$

Papers on these elements have already been published in the Physical Review.[1] In addition, $_{90}Th^{227}$, $_{91}Pa^{232}$, $_{91}Pa^{233}$, and $_{95}Am^{241}$ are presently being investigated at this laboratory, and future work on elements higher than curium in the periodic table is being contemplated.

The investigations carried out so far have only partially fulfilled the stated objectives. In each of these elements the g_J and J values

of the ground state have been measured, and from these it has been possible to formulate a general picture for the coupling of electrons in the heavy-element region. In addition, it has been possible to observe and to make these measurements on some of the excited states of curium. This led to a determination, from intensity considerations, of the energy-level splitting of the curium ground-state multiplet.

The nuclear ground-state spin has been measured directly for all these isotopes except curium. In Cm^{242}, the spin is believed to be zero, and very strong evidence can be obtained to support this belief. However, the atomic beam, like most other resonance techniques, can never be made to yield an unambiguous spin-zero measurement.

The hyperfine-structure separation has been determined for Pu^{239} The availability of wave functions for 5f electrons in the uranium atom has made possible the calculation of electronic matrix elements appropriate to the hyperfine-structure separation. By using these, it has been possible to infer the nuclear moment of Pu^{239} and to state crude lower limits to the moments of the neptunium isotopes.

The hyperfine structures of Np^{238} and Np^{239} afford the best opportunities of all those elements investigated to observe an octupole moment and perhaps a hexadecapole moment. This has not been done for two reasons. Intensity considerations makes it extremely difficult to observe resonances in the intermediate field region, because here only a single transition between two hyperfine-structure levels is observable to any one time. In the Zeeman region of hyperfine structure, where there is uniform splitting between the magnetic substates of a hyperfine-structure level, as many as eleven flop-in transitions are simultaneously observable in the $F = 8$ level of the electronic ground state of Np^{239}. To surmount this intensity problem a new atomic beam apparatus is planned.

The radiation hazard involved in the handling of the neptunium isotopes has also served to inhibit the measurement of their hyperfine structures. Although precautions have been taken to shield the body from high radiation dosages, the hands of necessity inevitably take a large dosage, amounting sometimes to several roentgens in a week of heavy running.

Before the main text of the thesis is commenced, two points seem worth making. The first concerns nuclear structure in the heavy elements. The author has tried to interpret the measurements made here and related data in the literature on the basis of the Nilsson model. Although enough data exist to make a relatively complete analysis of Pu^{239}, the sparsity of data on the neptunium isotopes makes for only a weak test of the Nilsson model. However, a measurement of the dipole and quadrupole moments of these isotopes along with the spins would make a very strong test.

The second point concerns the problem of symbols, which is always present in a long work. A unique (and wherever possible, the conventional) symbol has been used for each physical quantity. Hence if a symbol remains undefined in the text, it either has been defined elsewhere, or is so commonly used that a definition is felt to be unnecessary.

SPECULATIONS ON NUCLEAR AND ELECTRONIC STRUCTURE IN THE HEAVY ELEMENTS

Nuclear Structure

The breakdown of the single-particle model in which the last odd nucleons are assumed to move in a spherically symmetric potential provided by the nuclear core was first demonstrated by the observation of large quadrupole moments and isotope shifts in the rare earths.[2] It was pointed out by Rainwater that these effects could be explained on the assumption of a deformed nuclear core,[3] and from this notion has sprung up the so-called collective model.[4, 5]

The main point is that the core is now characterized by an ellipsoidal surface which can undergo oscillations. These oscillations are of two types; a type due to vibration around the equilibrium shape, and a type due to rotation of the system as a whole, preserving both the shape and internal structure of the core. The vibrational motion can be quantized according to standard field theoretic methods to yield surface vibrations known as surfons which carry angular momentum in units of $2\hbar$ and energy in units of $\hbar\omega$. The energy $\hbar\omega$ varies from 1 to 10 Mev, depending on the mass number A.[6] These energies are high enough that they will not in general influence the structure of the ground state and first few excited states.

The rotational motion is characterized by a moment of inertia $\mathcal{I}$, and has associated with it a rotational energy spectrum; the energy of the rotational levels is given by

$$E_{rot.} = \frac{\hbar^2}{2\mathcal{I}}\left[I(I+1)-I_0(I_0+1)+d\left\{(-)^{I+1/2}(I+1/2)-(-)^{I_0+1/2}(I_0+1/2)\right\}\right], \tag{I.1}$$

where I is the spin of the nuclear level, and I_0 is the spin of the nuclear ground state. The quantity d is called the decoupling parameter and is zero unless the odd nucleon lies in a state $\Omega = 1/2$. More will be said about this later.

The coupling of the nuclear core to the odd nucleon can be best considered from the point of view in which the nuclear core is regarded

as spherically symmetric in zeroth approximation, giving rise to a potential V(r). Therefore

$$\mathcal{H} = -\frac{\hbar^2}{2\mu}\nabla^2 + V(r). \qquad (I.2)$$

If the core is now permitted to assume the ellipsoidal shape described above, the zeroth-order potential will be modified by the addition of a term $\mathcal{H}_{int}$. The dynamic character of the potential due to core vibration can be neglected, since the motion of the particle is fast with respect to the vibrational frequency. Rotation will have no dynamic effect as we will henceforth assume the nuclear surface to be cylindrically symmetric. If the potential is expressed in a coordinate system fixed in the nucleus with z' the symmetry axis, then $\mathcal{H}_{int}$ can be shown[7] to have the form

$$\mathcal{H}_{int} = -E_1 \eta r^2 Y_{20}. \qquad (I.3)$$

Here E_1 is a constant that can be evaluated from the shell-model level structure, Y_{20} is the spherical harmonic of order two, and the quantity η is proportional to the deformation.

Using for V(r) a harmonic potential $\frac{1}{2}\omega r^2$ and including a spin-orbit potential $E_2 \vec{\iota} \cdot \vec{s}$, and a term $E_3(\vec{\iota})^2$ to depress in energy the states of high ι, Nilsson was able to calculate a set of energy levels and wave functions in terms of the parameter η where the wave functions are expressed in terms of the eigenstates of Eq. (I.2).[7] We may discuss these states in two coupling limits.

1. Strong Coupling

In this limit, that which is applicable in the heavy elements, η is large enough so that the spin-orbit coupling can be treated as a perturbation. The good quantum numbers in this situation are Ω, the component of the particle angular momentum along the nuclear symmetry axis, and π, the parity. Furthermore, since all the terms in the Hamiltonian are invariant with respect to reflection in a plane perpendicular to the nuclear symmetry axis, levels which differ only in the sign of Ω are

degenerate. Although $\mathcal{H}_{int}$ will couple levels in which N, the total oscillator quantum number, differs by two units, the spacing between successive N levels is wide enough so that the effect of this perturbation is negligible. Hence N and its component along the symmetry axis n_z are taken as good quantum numbers. Finally, so far as it is possible to neglect the spin-orbit term, Λ and Σ, the components of $\vec{\iota}$ and $\vec{s}$ along the symmetry axis are good quantum numbers (see Fig. 1 for a diagram of the various angular momenta and their relationships). A level in the strong-coupling approximation will henceforth be denoted by $(N, n_z, \Lambda, \pi)\Omega$.

The ground state of the nucleus is determined by successively filling up the levels in increasing energy. Since states of equal and opposite Ω are degenerate, the nucleons will pair off in these levels. Hence in even-even nuclei, the total $\Omega = 0$. For an odd-even nucleus the total Ω is either Ω_p or Ω_n of the last odd particle, proton or neutron. For these cases, the ground-state spin is just $I_0 = \Omega$ provided $\Omega \neq 1/2$. For the case $\Omega = 1/2$, the ground-state spin depends on the decoupling constant d. This occurs because for a state $\Omega = 1/2$, the intrinsic spin is partially decoupled from the rotational motion.[7] For odd-odd nuclei, the question of the ground-state spin has recently been investigated by Gallagher and Moszkowski.[8] These authors propose an extension of the Nordheim rules under the assumption that Λ and Σ are separately good quantum numbers. Under these conditions, they arrive at the coupling rules:

$$I_0 = \Omega_p + \Omega_N \quad \text{if} \quad \Omega_p = \Lambda_p \pm 1/2 \quad \text{and} \quad \Omega_N = \Lambda_N \pm 1/2,$$

$$I_0 = |\Omega_p - \Omega_N| \quad \text{if} \quad \Omega_p = \Lambda_p \pm 1/2 \quad \text{and} \quad \Omega_N = \Lambda_N \mp 1/2.$$

Magnetic moments in the strong-coupling approximation arise from the coupling, in odd A nuclei, of the moment of the odd particle with the moment of the core: (I.4)

$$\vec{\mu}_{op} = q_s \vec{s} + g_\iota \vec{\iota} + g_R \vec{R}, \qquad \text{(I.5)}$$

where $\vec{R}$ is the angular momentum of the core, and g_R, the g factor of the core,

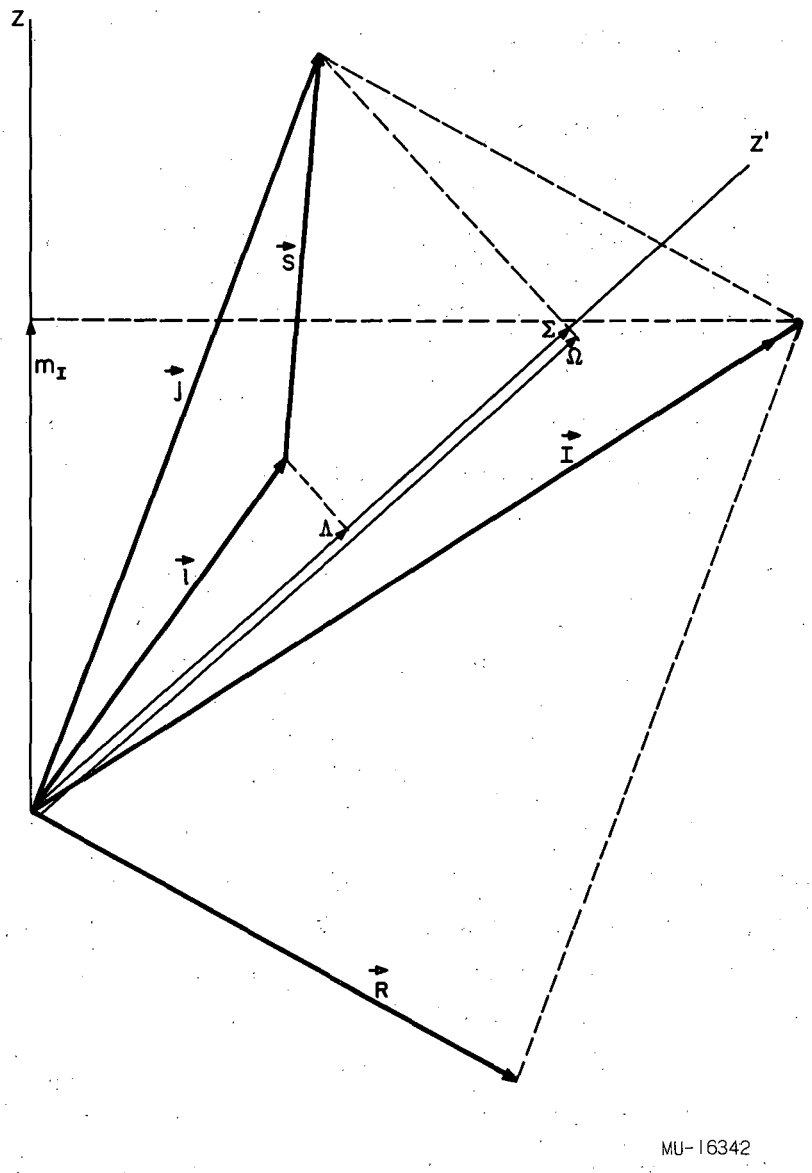

Fig. 1. Angular momentum relationships on the collective model.

is generally taken to be about Z/A. The matrix elements of this operator have been evaluated by Nilsson.[7] Hence if the deformation is known, the moment can be calculated from the wave functions.

Other aspects of the strong-coupling theory are not directly related to this work and are summarized elsewhere.[9]

2. Weak Coupling

This limit occurs near closed shells and is characterized by the predominance of the spin-orbit energy over $\mathcal{H}_{int}$. Since it is not applicable to this work, only the problem of the ground-state spin will be mentioned.

In this limit, the individual particle levels can be characterized by N, j, ℓ, s, Ω, and π. Particles will fill successively the substates of equal and opposite Ω belonging to a given j state. The ground-state spin for nuclei having one or two nucleons outside a closed shell and in the same j state is just $I_0 = j$, as in the shell model. For three such particles, however, the ground state is either j or $j-1$, depending on the deformation. Both these cases have been observed experimentally.

Electronic Structure

From 1923 through 1941, many papers appeared suggesting that electrons should start filling up the 5f level before completion of the 6d level, with a wide variety of suggestions for the element at which this transition series begins.[10] The impetus given by the war to heavy-element research has resulted in a great deal of chemical information bearing on the problem of the configuration of the electronic ground state. This evidence has been summarized by Seaborg.[11] Table I is a list of suggested electronic configurations in the heavy elements prepared by Seaborg on the basis of the evidence.[11]

Table I

Suggested electronic configurations (after Seaborg)

Element	Configuration
89– Ac	$6d\ 7s^2$
90– Th	$6d^2\ 7s^2$ or $5f\ 6d\ 7s^2$
91– Pa	$5f^2\ 6d\ 7s^2$ or $5f\ 6d^2\ 7s^2$
92– U	$5f^3\ 6d\ 7s^2$
93– Np	$5f^5\ 7s^2$ or $5f^4\ 6d\ 7s^2$
94– Pu	$5f^6\ 7s^2$
95– Am	$5f^7\ 7s^2$
96– Cm	$5f^7\ 6d\ 7s^2$
97– Bk	$5f^9\ 7s^2$
98– Cf	$5f^{10}\ 7s^2$
99–E	$5f^{11}\ 7s^2$
100–Fm	$5f^{12}\ 7s^2$
101–Mv	$5f^{13}\ 7s^2$
102	$5f^{14}\ 7s^2$
103	$5f^{14}\ 6d\ 7s^2$

THEORY OF EXPERIMENT

Hyperfine Structure

The subject of hyperfine structure has received the attention of many authors in the past thirty years.[12] Excellent summaries can be found in the literature. This section contains a detailed description of those aspects of hyperfine structure which are directly connected with the work in the transuranic region.

An atomic energy level which is characterized by a value J of the electronic angular-momentum quantum number is split by the hyperfine-structure interaction into substates according to the value of the total angular momentum $\vec{F}=\vec{I}+\vec{J}$, where $\vec{I}$ is the angular momentum of the nucleus. The number of such substates is either $2I+1$ or $2J+1$, whichever is smaller. In the presence of an external magnetic field, a level of given F is in turn split in energy into $2F+1$ further substates, each characterized by a different possible value of m_f, the z component of the total angular momentum.

The physical origin of hyperfine structure is the noncentral part of the electromagnetic interaction between electrons and a nucleus of finite extent. Quantum-mechanically, the interaction Hamiltonian is

$$\mathcal{H}_{hfs} = ha\,(\vec{I}\cdot\vec{J}) + \frac{hb}{2I(2I-1)J(2J-1)}\left[3(\vec{I}\cdot\vec{J})^2 + 3/2(\vec{I}\cdot\vec{J}) - I(\vec{I}+1)J(J+1)\right]$$

$$+ \frac{5}{4}\,hc\,\frac{(\vec{I}\cdot\vec{J})^3 + 4\,(\vec{I}\cdot\vec{J})^2 + 4/5(\vec{I}\cdot\vec{J})\left[-3I(I+1)J(J+1)+J(J+1)+3\right] - 4I(I+1)J(J+1)}{I(I-1)(2I-1)J(J-1)(2J-1)}$$

$$+\ldots. \qquad \text{(II.1)}$$

where h is Planck's constant. The normalization used here with respect to the interaction constants $a, b, c, \ldots$ is the same as that given by Ramsey.[13] The term in a arises from the interaction of the magnetic dipole moment of the nucleus with the magnetic field of the electrons at the nucleus. The term in b is the electric quadrupole interaction, that in c is the magnetic octupole interaction, etc. If successive terms in

the series are denoted as 2^k (k=1, 2, 3, . . . etc.) pole interactions, then the highest-order term k present in the series is either 2I or 2J, whichever is smaller. The order of magnitude of the ratio of successive magnetic-interaction constants and successive electric-interaction constants can be estimated from hyperfine-structure theory to have the form $\frac{Z^2}{10}\left(\frac{R_n}{a_0}\right)^2$. The factor 1/10 is somewhat arbitrary and arises from the fact that the ratio of the matrix elements of $(1/r)^{n+2}$ and $(1/r)^n$ involve normalization factors of this order of magnitude. The dependence on Z, R_n, and a_0 is pretty well established—at least theoretically. Some predicted octupole interaction energies found by using this formula and the measured dipole constants are:

	Predicted (kc)	Measured (kc)
Ga^{69}	0.17	0.08
Ga^{71}	0.22	0.12
In^{115}	0.76	1.1
In^{127}	2.8	2.3

The measured values are those as corrected by Schwartz[14] for electronic perturbations. This effect will be described in what follows.

On the basis of the above approximation, predictions of higher-order multipole interactions in the heavy elements can be attempted. In Np^{239}, for instance, the dipole interaction is known to be at least 20 Mc so that an estimate of the lower limit of the octupole interaction is 0.4 kc. Another way to say this is that there is about 1 kc of magnetic octupole or electric hexdecapole interaction per 50 Mc of magnetic dipole or electric quadrupole interaction. Hence, there is a fair possibility that one or both of these effects is measurable in some of the heavy elements.

An important point connected with the measurement of higher-order multipole interactions is that if one wishes to determine the pure nuclear 2^k pole interaction then one must separate out that part of the interaction energy which is due to second-order effects of combined k'

and k-k' interactions where k' is any integer less than k, (Schwartz correction mentioned above). For example, an octupole-like splitting in the hyperfine structure arises from the coupling of the dipole and quadrupole interactions of states of the same F but different J. This effect can not be separated experimentally from the measured energy, but must be calculated from known atomic wave functions. It is worth while to emphasize that the effect of electronic perturbations can be large enough to seriously enhance or negate the nuclear octupole effect. In the isotope In^{115}, for example, the effect due to perturbation is as large as the nuclear effect and opposite in sign so that the observed effect is zero.

The foregoing represents in brief the basis for the measurement of higher-order nuclear multipole moments and some of the pitfalls involved. A more detailed treatment will await actual measurement.

Hyperfine-structure measurements made in these experiments involve the observation of $\Delta F=0$ transitions in the presence of both weak and strong external fields. Occasional observations were made of $\Delta F = \pm 1$ transitions in the presence of weak external fields in connection with direct observation of hyperfine-structure splittings. The presence of an external field gives rise to a Hamiltonian,

$$\mathcal{H} = \mathcal{H}_{hfs.} - g_J \mu_0 J_z H_0 - g_I \mu_0 I_z H_0, \qquad (II.2)$$

$$(g_J < 0 \text{ for electrons})$$

where $\mathcal{H}_{hfs}$ is stated in Eq. (II.1), g_J and g_I are the electronic and nuclear g factors respectively, and μ_0 is the Bohr magneton. The direction of the field H_0 is taken to be the z direction. The splitting of the levels characterized by the quantum numbers I, J, F, m_f is then determined from the energy matrix. If we neglect off-diagonal terms in J, then the only off-diagonal elements present arise from the matrix elements of J_z and I_z which couple the states $|F, m_f\rangle$ with the states $|F+1, m_f\rangle$ and $|F-1, m_f\rangle$. Hence the energy matrix will have the form shown on the following page.

	$m_f = F_m$	$m_f = F_m - 1$	$m_f = F_m - 2$	...	$m_f = -F_m$
$m_f = F_m$	$\langle F_m \mid \mathcal{H} \mid F_m \rangle$	0	0	...	0
$m_f = F_m - 1$	0	$\begin{pmatrix} \langle F_m \mid \mathcal{H} \mid F_m \rangle & \langle F_m - 1 \mid \mathcal{H} \mid F_m \rangle \\ \langle F_m \mid \mathcal{H} \mid F_m - 1 \rangle & \langle F_m - 1 \mid \mathcal{H} \mid F_m - 1 \rangle \end{pmatrix}$	0	...	0
$m_f = F_m - 2$	0	0	$\begin{pmatrix} \langle F_m \mid \mathcal{H} \mid F_m \rangle & \langle F_m - 1 \mid \mathcal{H} \mid F_m \rangle & 0 \\ \langle F_m \mid \mathcal{H} \mid F_m - 1 \rangle & \langle F_m - 1 \mid \mathcal{H} \mid F_m - 1 \rangle & \langle F_m - 2 \mid \mathcal{H} \mid F_m - 1 \rangle \\ 0 & \langle F_m - 1 \mid \mathcal{H} \mid F_m - 2 \rangle & \langle F_m - 2 \mid \mathcal{H} \mid F_m - 2 \rangle \end{pmatrix}$	...	0
.....	...	.....	.....	...	...
$m_f = -F_m$	0	0	0	...	$\langle F_m \mid \mathcal{H} \mid F_m \rangle$

Here we have $F_m = I+J$, and only the value of F appears in the label of the states in the above matrix. The process of diagonalization of the energy matrix consists, therefore, of diagonalizing the individual submatrices corresponding to different values of m_f. It is apparent that, in general, this necessitates evaluating the roots of polynomial expressions of arbitrary order.

To surmount these complex computational problems, a routine has been set up for the IBM 650 computer.[15] Given the state for which the energy is desired (i.e., I, J, F, m_f), the computer will calculate the elements of the submatrix corresponding to the given value of m_f, retaining only the terms in a and b in $\mathcal{H}_{hfs}$. It will then solve the polynomial expression resulting from the diagonalization of the submatrix for the particular root appropriate to the state F desired. The restriction on I and J is that the smaller of the two be less than 19/2. This routine is proving particularly useful in the work currently being carried out on Am^{241}, where I=5/2 and J=7/2.

While the solution in the general case of the energy levels of the Hamiltonian Eq. (II.2), is possible only numerically, the same problem for the case in which either I or J is 1/2 is easily solved in analytic form. In that case $\mathcal{H}_{hfs} = a\vec{I}\cdot\vec{J}$, and

$$\mathcal{H} = ha\,\vec{I}\cdot\vec{J} - g_J\mu_0 J_z H_0 - g_I\mu_0 I_z H_0 . \qquad \text{(II.3)}$$

Only two F levels are present here; in the case J=1/2 they are I-1/2 and I+1/2. Hence the energy matrix for the state m_f is of the form on the following page.

The quadratic equation that results from diagonalization can be solved to yield the energy levels.

$$W = -\frac{\Delta W}{2(2I+1)} - g_I\mu_0 m_f H_0 \pm \frac{\Delta W}{2}\left[1 + \frac{4m_f x}{2I+1} + x^2\right]^{1/2} \qquad \text{(II.4)}$$

$$\Delta W = ha\,\frac{2I+1}{2} \qquad x = \frac{(g_I - g_J)\,\mu_0 H_0}{\Delta W}$$

	F = I+1/2	F = I-1/2
F = I+1/2	$\frac{haI}{2} - \frac{\mu_0 H_0 m_f}{2I+1}(2g_I I+g_J)$	$-\frac{\mu_0 H_0 (g_I-g_J)}{2I+1}\sqrt{(I+1/2)^2-m_f^2}$
F = I - 1/2	$-\frac{\mu_0 H_0 (g_I-g_J)}{2I+1}\sqrt{(I+1/2)^2-m_f^2}$	$-\frac{ha}{2}(I+1)-\frac{\mu_0 m_f H_0}{2I+1}\left[2g_I(I+1)-g_J\right]$

This derivation was first performed by Breit and Rabi.[16] The positive sign refers to the state $|F=I+1/2, m_f\rangle$ and the negative sign to $|F=I-1/2, m_f\rangle$. Figure 2 is a plot of W/a vs x for K^{39}, which is characterized by J=1/2, I=3/2.

A particularly simple solution of the Hamiltonian (II.2) is obtainable in the two limits $x \ll 1$ and $x \gg 1$ (weak and strong field respectively). In the weak-field case we start with the zero-field energy levels, i.e., the solutions to the Hamiltonian $\mathcal{H}_{hfs}$. In the absence of external field, the physical picture describing the situation is that the nuclear and electronic angular momenta couple together to form the total angular momentum $\vec{F}$. The hyperfine-structure interaction causes the electronic and nuclear magnetic moments to precess about the vector $\vec{F}$. Hence the components of the moments perpendicular to $\vec{F}$ average to zero and the effective component of the moment ($\vec{\mu}_{eff}$) is the component along F:

$$\vec{\mu}_{eff} = g_J \mu_0 \frac{\vec{J}\cdot\vec{F}}{(\vec{F})^2}\vec{F} + g_I \mu_0 \frac{\vec{I}\cdot\vec{F}}{(\vec{F})^2}\vec{F} \qquad \text{(II.5)}$$

The weak external field $\vec{H}_0$ does not destroy this coupling. Rather, this field causes the total coupled system $\vec{\mu}_{eff}$ to precess about $\vec{H}_0$. Therefore, the additional energy imposed on the system is

$$W = -\vec{\mu}_{eff}\cdot\vec{H}_0 = -(g_J\vec{J}\cdot\vec{F} + g_I\vec{I}\cdot\vec{F})\mu_0\frac{\vec{F}\cdot\vec{H}_0}{(\vec{F})^2} \equiv g_F\mu_0 m_f H_0 ,$$

$$\therefore \quad g_F = -g_J\frac{F(F+1)+J(J+1)-I(I+1)}{2F(F+1)} - g_I\frac{F(F+1)+I(I+1)-J(J+1)}{2F(F+1)} . \qquad \text{(II.6)}$$

The ratio g_I/g_J is of order m_e/m_p (electron mass/proton mass) and in practice it is usually convenient to neglect the g_I term. The difference in energy of two states belonging to the same F for which m_f differs by one is, in this approximation,

$$\Delta W = -g_J\frac{F(F+1)+J(J+1)-I(I+1)}{2F(F+1)}\mu_0 H_0 . \qquad \text{(II.7)}$$

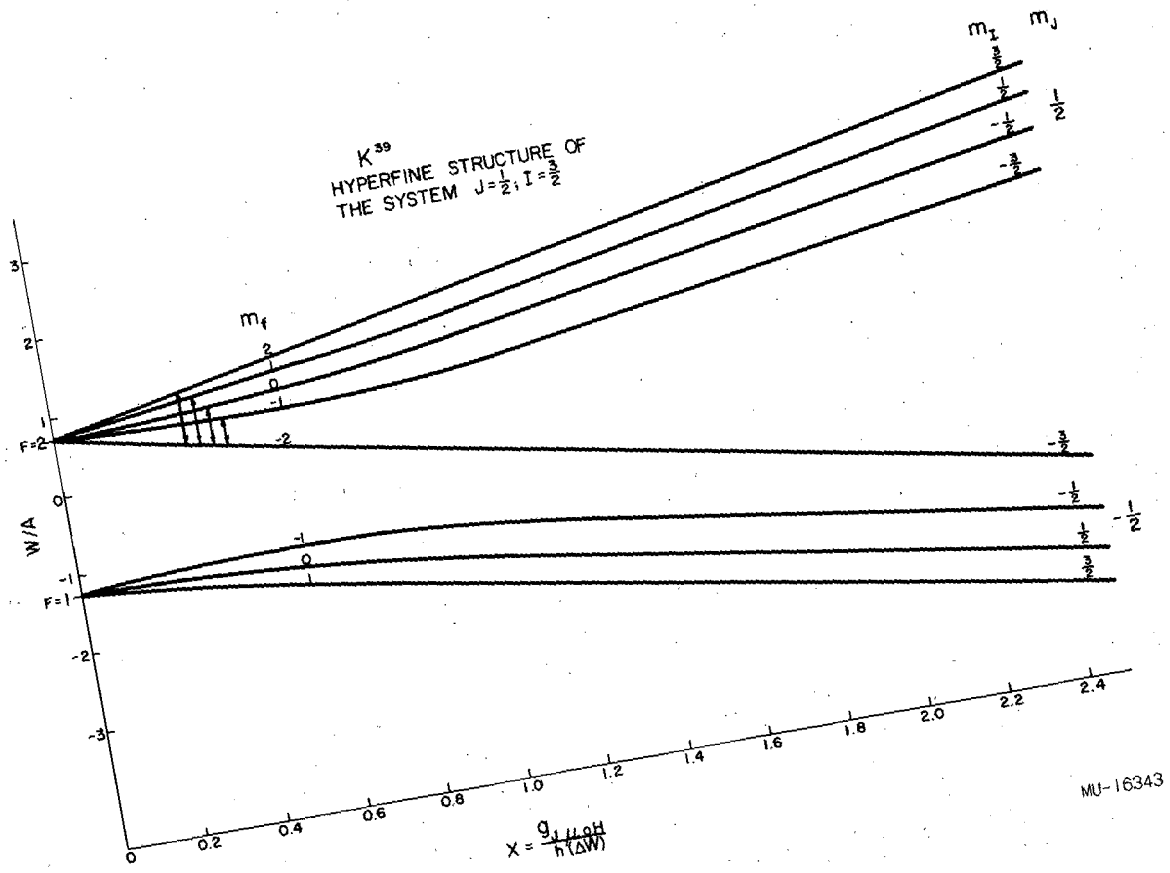

Fig. 2. Energy levels of the system I = 3/2, J = 1/2 in a magnetic field.

Equation (II.7) gives us the basis for determining nuclear spins from weak-field or Zeeman measurements. In the transuranic elements, the quantities I, J, F, and g_J were all unknown prior to this research for the neptunium isotopes and for Cm^{242}. The nuclear spin had already been established for Pu^{239}. The method for fixing each of the unknowns is discussed for each element investigated in the section pertaining to that element.

For strong fields, the physical situation is described by depicting the nuclear and electronic moments as sufficiently decoupled so that they precess separately about the applied external field. Hence, all components average to zero except those along the field direction. If we notice that $\mathcal{H}_{hfs}$ is a function only of $\vec{I} \cdot \vec{J}$, then in the strong-field limit we obtain the diagonal elements of this operator by replacing $\vec{I} \cdot \vec{J}$ everywhere by $m_I m_J$. For example, the strong-field solution to the Hamiltonian for I or J equal to 1/2 is

$$\mathcal{H} = ham_I m_J - g_I \mu_0 m_I H_0 - g_J \mu_0 m_J H_0. \qquad \text{(II.8)}$$

Note that the levels are linear in the field and that for $g_I \mu_0 m_I H_0 < ham_I m_J$ (the usual laboratory strong-field case) states of positive m_I have higher energy for positive m_J, whereas for negative m_J, states of negative m_I will have higher energy. These features are exhibited by the hyperfine structure of K^{39} (Fig. 2). Measurement of the slope of the high-field levels is an accurate way to obtain the value of g_J.

A primary problem in the theory of hyperfine structure is to determine the explicit dependence of the interaction constants a, b, c, . . . , etc. on the appropriate electronic and nuclear matrix elements. The evaluation of the constant a is pertinent to the work described here, so that nuclear dipole moments can be inferred from the empirically measured values. The evaluation of the constant a was first done correctly by Fermi[17] for the case of a single electron in a ^2S state. In his calculation, Fermi treated the nucleus as a point dipole, and the electron as a relativistic particle obeying the Dirac equation. This treatment yielded the celebrated Fermi formula for the hyperfine structure,

$$ha = \frac{16\pi}{3}\left(\frac{\mu_L}{I}\right)\mu_0 \left|\psi_n(0)\right|^2 . \qquad \text{(II.9)}$$

Small corrections to this formula arising from quantum electrodynamics,[18] relativistic mass shifts,[19] and the anamolous magnetic moment of the electron.[20] have all been calculated to bring Eq. (II.9) into complete agreement with the observed hyperfine structure of hydrogen.[21] Semi-empirical methods have been devised for the evaluation of $\left|\psi_n(0)\right|^2$ so that Eq. (II.9) can be applied to the alkalis.[22]

A very fruitful method for the derivation of the form of the interaction constant a in non-s states can be obtained by writing

$$ha\vec{I}\cdot\vec{J} = -\vec{\mu}_I\cdot\vec{H}, \qquad \text{(II.10)}$$

where $\vec{H}$ is the magnetic field at the nucleus due to the orbital electrons. Starting from the classical expression for $\vec{H}$ one can then derive the expression for a single electron in non-s states.[23] This yields

$$ha = 2\left(\frac{\mu_I}{I}\right)\mu_0\left\langle\frac{1}{r^3}\right\rangle\frac{L(L+1)}{J(J+1)} . \qquad \text{II.11)}$$

Finally, the same treatment can be extended to the case of n equivalent electrons in a non-s state. The expression for the resultant interaction is

$$ha = 2\left(\frac{\mu_I}{I}\right)\mu_0\left\langle\frac{1}{r^3}\right\rangle\left\{\frac{J(J+1)+L(L+1)-S(S+1)}{2J(J+1)}\right.$$

$$+\frac{2(2L-n^2)}{n^2(2L-1)(2l-1)(2l+3)}\left[\frac{L(L+1)\left[J(J+1)+S(S+1)-L(L+1)\right]}{2J(J+1)}\right. \qquad \text{(II.12)}$$

$$\left.\left.-\frac{3}{4}\frac{\left[J(J+1)-(L(L+1)-S(S+1)\right]\left[J(J+1)+L(L+1)-S(S+1)\right]}{J(J+1)}\right]\right\}$$

This formula is derived in the limit of pure L-S coupling between the individual electrons according to Hund's Rule. The notation is used that l is the orbital angular-momentum state of the individual electrons, L and S are respectively the total orbital and spin angular momenta of the coupled electrons, and $J = \left|\vec{L}+\vec{S}\right|$ is the total angular momentum. That this formula reduces to Eq. (II.11) in the case n = 1, S = 1/2 is easily verified.

Theory of the Resonance Process

The method used in these experiments is the atomic-beam flop-in method first proposed by Zacharias[24] as a modification of Rabi's original resonance proposal.[25] The essential point of this technique is that with the field gradients in the A and B magnets aligned (see Fig. 3), no atom can be deflected around the stop wire (S) so as to reach the detector (D) unless its magnetic moment has changed sign in the region of the homogeneous C field.

In detail, the resonance process occurs in the following fashion. An atom effusing out of the oven slit in the forward direction enters the region of the A magnet and undergoes deflection. In the homogeneous C field it moves linearly, but if it has a nonzero magnetic moment the atom precesses about the field with the Larmor frequency $\omega_0 = \frac{\mu H_0}{F\hbar}$. The oscillatory field, which is then at right angles to the homogeneous field, exerts a torque on the atom, $\tau = \vec{\mu} \times \vec{H}_1$. Let us consider the linearly polarized oscillatory field to be composed of two circularly polarized components, one rotating in the same direction as the precession of the atom (positively) and the other rotating in the opposite direction (negatively). Speaking classically, we can say that if the positively rotating component has a frequency far from the Larmor frequency, then, over many rotations of the atom about the C field, the average value of the torque exerted by the oscillatory field is zero. However, close to the Larmor frequency, the time average is nonzero, and after the atom has traversed the C field there is, in general, a change in azimuthal orientation of the magnetic moment. Quantum-mechanically, of course, the new orientations are restricted to the possible substates of the angular-momentum vector. If the final orientation is opposite to the initial orientation, so that the magnetic moment in the B magnet is equal in magnitude and opposite in direction to that in the A magnet, then the atoms passing through the collimating slits can be deflected around the stop wire and be collected on the detector. From this picture of the resonance process, formulas can be derived for the shape and height of resonance curves. The shape of resonance curves (intensity vs frequency near the resonant frequency)

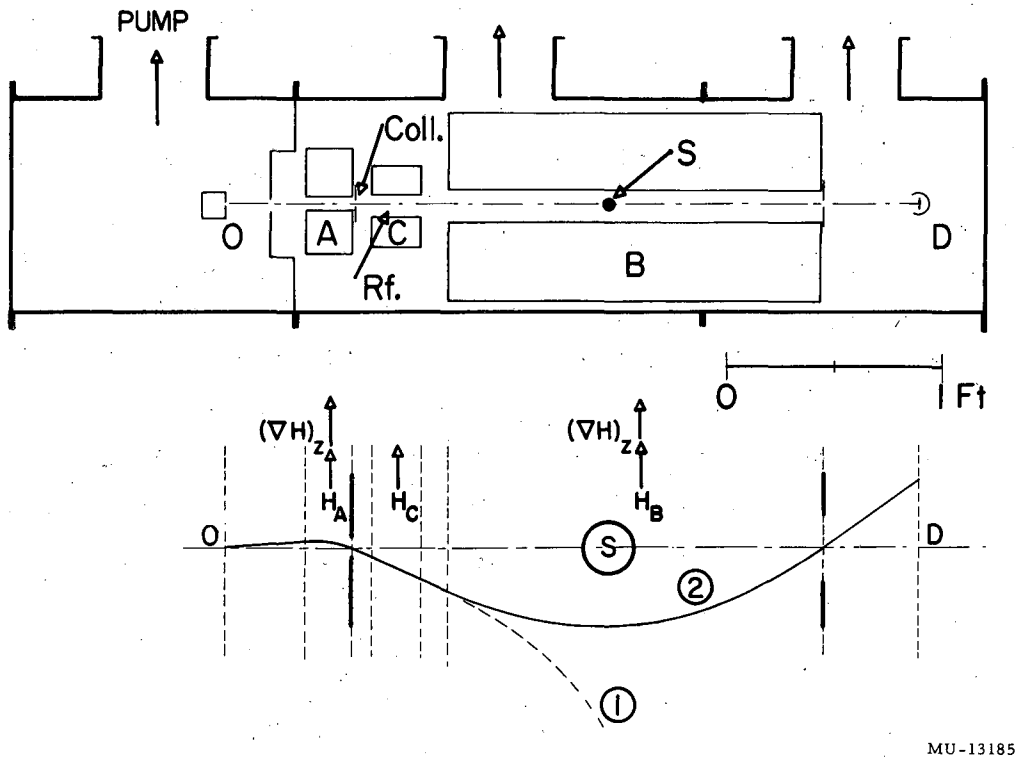

Fig. 3. Schematic arrangement and trajectory in an atomic-beam flop-in apparatus.

is considered in detail by Ramsey.[13] The height of a resonance at the resonant frequency becomes important in the researches on the neptunium isotopes and curium.

Resonance Height

The intensity (i) at resonance at the detector for a given transition in an atomic-beam flop-in-type experiment can be thought of as proportional to the product of three factors,

$$i = CNPA,$$

where C is a normalizing constant, N is the population of the magnetic substate undergoing transition, P is the probability of transition from initial to final state, and A is an apparatus factor.

The population per magnetic substate N is simply given by the Boltzmann factor, $N = \exp(-E/kT)$, where E is the energy of the state.

The transition probability P between two magnetic substates m_f, m'_f of a level of given total angular momentum F under the action of an applied radio-frequency field was first derived by Majorana.[26] This derivation assumes that the full effect of the rf is felt instantaneously at t = 0. Explicitly, this transition probability is given by

$$P_F^{m_f, m'_f} = (F-m_f)!\ (F-m'_f)!\ (F+m_f)!\ (F+m'_f)!\ \sin^{4F}\left(\frac{a}{2}\right)\left[\sum_r \frac{(-)^r \cot^{m_f+m'_f+2r}\left(\frac{a}{2}\right)}{(F-m_f-r)!\,(F-m'_f-r)!\,(m_f+m'_f+r)!\,r!}\right]^2 \qquad \text{(II.13)}$$

The transition is from the state F, m_f to the state F, m'_f, and the sum is over all values of r that keep the factorials positive. Here, we have

$\sin^2 \frac{a}{2} = P_{1/2}^{1/2,\,1/2}$, where $P_{1/2}^{1/2,\,1/2}$ is the transition probability for a moment with the same gyromagnetic ratio, but a spin of 1/2. This is given by

$$P_{1/2}^{1/2,\,-1/2} = \frac{(2b)^2}{(\omega-\omega_0)^2 + (2b)^2} \sin^2 1/2\left[(\omega-\omega_0)^2 + (2b)^2\right]^{1/2} t. \qquad \text{(II.14)}$$

In this formula, ω is the applied frequency, ω_0 is the Larmor precession frequency of the atom in the homogeneous C field; b is the interaction energy of the moment with the transition field, i.e., $b = \frac{\mu H_1}{2h}$, where H_1 is the amplitude of the oscillatory field; and the factor 2 comes from the fact that only the circularly rotating part of the field in the direction of precession of the atom causes transitions. The length of time the atom spends in the transition region is denoted by t.

In this work, the only case of interest was the transition probability for $\omega = \omega_0$. At this frequency, we have, for $P_F^{m_f, m'_f}$,

$$P_F^{m_f, m'_f} = (F-m_f)!\,(F-m'_f)!\,(F+m_f)!\,(F+m'_f)!\,\sin^{4F}\left(b\frac{\ell}{v}\right) \times \left[\sum \frac{(-)^r \cot^{m_f+m'_f+2r}\left(\frac{b\ell}{v}\right)}{r!\,(F-m_f-r)!\,(F-m'_f-r)!\,(m_f+m'_f+r)!\,r!}\right]^2, \qquad \text{(II.15)}$$

where ℓ = length of transition region,

v = velocity of atom in the beam.

In order to apply Formula (II.15) to any practical cases, consideration must be given the fact that there is present in the beam a distribution of velocities, and that the probability of an atom having a velocity between v and v+dv is given by

$$I(v) = \frac{2}{a^4}\, v^3 \exp\left(-v^2/a^2\right), \qquad \text{(II.16)}$$

where a = the most probable velocity in a Maxwell-Boltzmann distribution at the same temperature: $a = (2kT/m)^{\frac{1}{2}}$ Averaging Formula (II.15) over the velocity distribution involves the evaluation of integrals of the form

$$\int_0^\infty \sin^m\left(\frac{b}{v}\right) \cos^n\left(\frac{b}{v}\right) v^3 \exp(-v^2/a^2)\,dv, \qquad \text{(II.17)}$$

where m and n are integers. Such integrals can be evaluated quickly and accurately on the IBM 650 computer.

In order to have a detailed check of the applicability of the Majorana theory to these experiments, this evaluation was done for the flop-in transitions of K^{39}. The intensity at resonance in the F = 2 state of this isotope (see Fig. 2 for a hyperfine-structure diagram of this isotope) was measured as a function of rf current (Fig. 4). This curve was taken in the Zeeman region, where we are observing the transitions F=2: $m_f=-2 \leftrightarrow m_f=2$, $m_f=-2 \leftrightarrow m_f=1$, $m_f=-2 \leftrightarrow m_f=0$, $m_f=-2 \leftrightarrow m_f=-1$ all at once. A calculation was made of the transition probability averaged over the atomic-beam velocity distribution for each of these transitions for several values of the parameter $(b/a)^2$. $_{m_f, m_f=-2}$ The observed intensity should be proportional to the quantity $\sum_{m_f=-1}^{2} \overline{P}_2$, where the notation $\overline{P}$ indicates average value. This quantity is plotted as a function of $(b/a)^2$ in Fig. 4. A comparison with the experimental results was made by superimposing the experimental and theoretical curves (Fig. 5). Superimposing in this way allows an arbitrary choice of scale factor and normalization factor. These are chosen so as to make agreement between the two curves as close as possible.

The apparatus factor (A) arises from the fact that the deflecting power of the magnets is dependent on the magnetic moment of the atom. It is easy to see that very-low-energy and very-high-energy atoms can not reach the detector. Very-low-energy atoms are deflected into the magnet walls before they get very far down the apparatus, and very fast atoms are not deflected enough for their paths to be bent around the stop wire. Hence the apparatus geometry and the strength of the magnetic fields permits only a selected velocity band to be focused. The width of this band is, of course, dependent on the magnetic moment. It is easy to show that if we neglect the lower velocity limit, then the fraction of atoms that gets focused is given by $(1-e^{-v_c^2/a^2})$, where v_c is a velocity dependent on the parameters mentioned above. A derivation of this expression was first given by Sunderland.[27] He shows

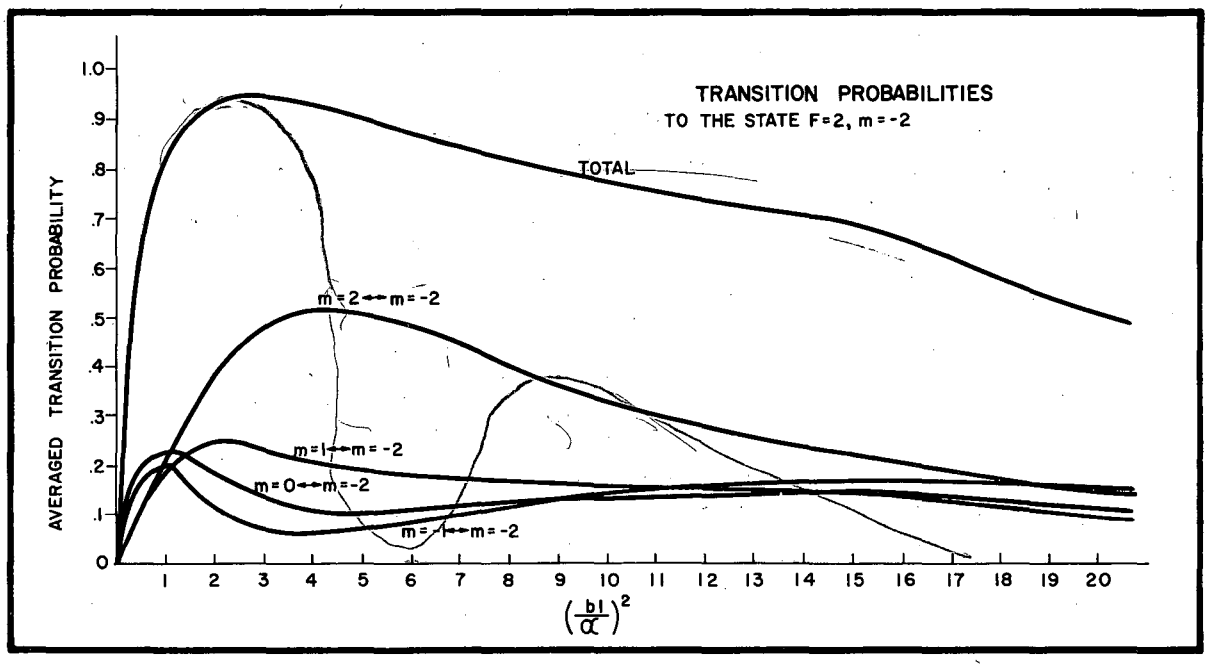

MU-16344

Fig. 4. Transition probabilities in K^{39}.

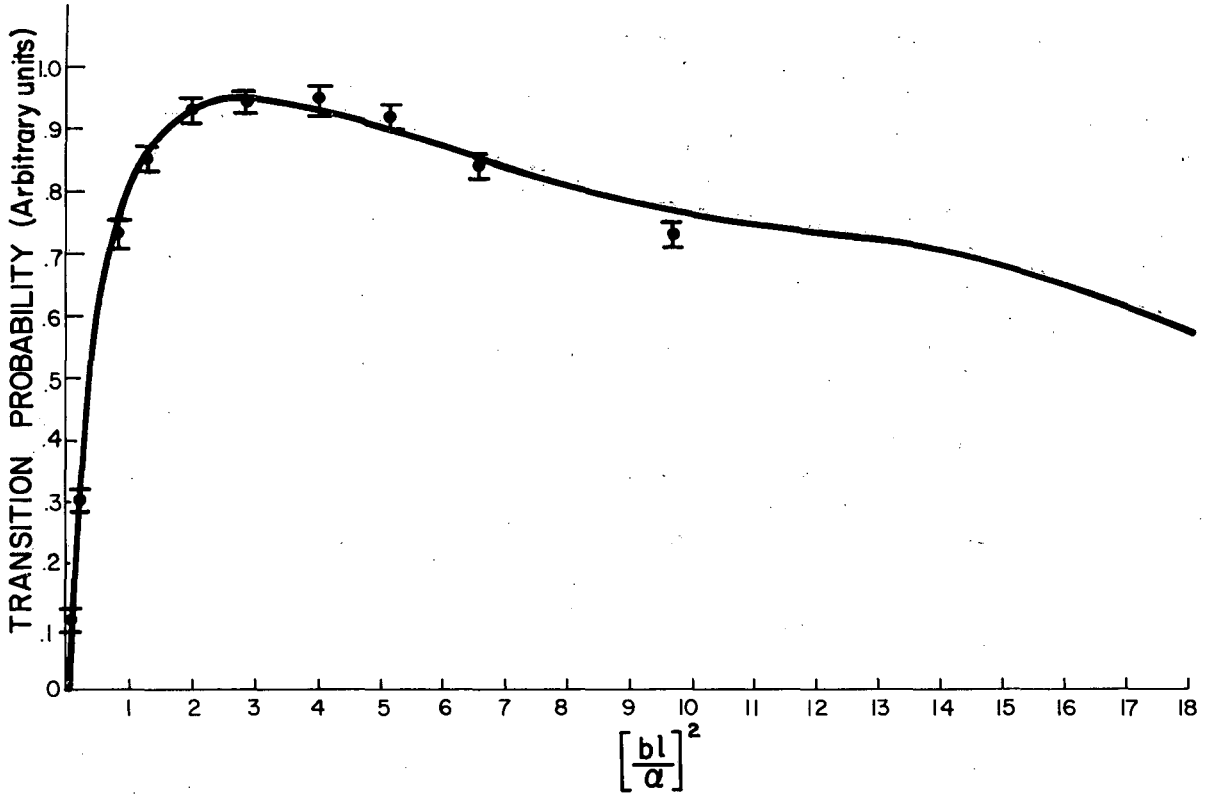

MU-16345

Fig. 5. Comparison of experimental observations and theoretical transition probabilities in K^{39}.

$$v_c = \sqrt{\frac{\mu}{m}} \left(C_1 \frac{\partial H_A}{\partial y} + D_1 \frac{\partial H_B}{\partial y} \right)^{1/2}, \qquad \text{(II.18)}$$

where $\frac{\partial H_A}{\partial y}$ and $\frac{\partial H_B}{\partial y}$ are the field gradients in the A and B magnets. C_1 and D_1 are factors which depend only on the apparatus geometry. Far away from magnet saturation, we can write $\frac{\partial H_A}{\partial y} \propto i_M$; $\frac{\partial H_B}{\partial y} \propto i_M$ where i_M is the magnet current. Therefore, $v_c = (C\mu i_M/m)^{1/2}$. Also, since $a = (2kT/m)^{1/2}$, then the expression for the intensity is $i = i_0\left[1-\exp\left(-C\frac{\mu}{T} i_M\right)\right]$. This relation can be checked experimentally by varying the current in the A and B magnets and measuring the intensity at resonance. This was done for K^{39} with the result that an approximately exponential curve was obtained. If we use this curve to yield a value for C, we obtain
$C = 1.2 \times 10^{24} (\text{erg-cm}/^{\circ}\text{K})^{-1}$.

EXPERIMENTAL METHOD

It was stated in the section on the theory of experiment that the determination of the electronic and nuclear constants of an atomic system involves the determination of the resonant frequencies of the system at particular settings of the homogeneous C field. The great accuracy obtainable with the atomic-beam technique is made possible by the fact that measurements of only a magnetic field and a frequency are necessary in any experiment. In this section the procedure and equipment involved in these measurements is discussed.

Running Procedure

Once the preliminary chemistry has been done on the material under investigation, it is placed in a small oven. The oven is in turn mounted in an oven loader designed to permit rapid positioning of the oven in the apparatus with minimum disturbance to the apparatus vacuum. The oven is then optically aligned so that the aperture out of which the beam effuses is collinear with the magnet gap (see Fig. 3 for a schematic diagram of the apparatus). It is advisable at this point to set the C field to the desired value. An accurate calibration of the field is made possible by the fact that the hyperfine-structure constants of K^{39} are accurately known.[28] Since $J = 1/2$ for the ground state of K^{39} the energy levels as a function of field obey the Breit-Rabi Equation (II.4), and the transition frequency for a desired field setting may be calculated to an accuracy greater than the resolution of the apparatus. Hence the C field may easily be set by setting the oscillator that drives the rf hairpin at the appropriate frequency, and then varying the current through the C magnet coils until the resonance is observed. The value of the C field is conveniently expressed in terms of the quantity $\frac{\mu_0 H_0}{h}$ in Mc. This will usually be used in the text, instead of stating H_0 in gauss. The adjustability of the field for fields below about 20 Mc is limited by the resonance line width of about 25 kc, and is about one part per 1000 for fields above 20 Mc.

After the field is set, the oven is then heated to a sufficient temperature to establish an adequate beam at the detector. In the heavy elements, beam temperatures vary from 900°C to 3000°C, depending on

the material. When the beam temperature is reached, a resonance exposure is then taken. This involves setting the oscillator to a particular frequency and allowing the beam to pass down the apparatus for 5 or 10 minutes and to impinge on the detector. At the end of this time the detector is removed and placed in an appropriate radiation counter. Meanwhile, the oscillator is set to a new frequency and the procedure is repeated. In general, the field setting and beam intensity are checked between resonance exposures.

Experimental Apparatus

The physical construction of the atomic-beam machine used in these experiments has been described elsewhere.[29] Only new features and features that have undergone modification are discussed here.

1. Ovens

The necessity of obtaining temperatures up to 3000°C places severe restrictions on the possible oven materials. The further requirement of obtaining these temperatures with a reasonable power, using the electron-bombardment technique, necessitates that the oven size be kept small and that the oven be mounted in such a way that heat transfer to the surroundings be minimized. Finally, the oven material used must be free from interaction with the material under investigation at beam temperatures. Up to the present, the material most satisfactory from these points of view is tantalum (mp = 3000°C). Ovens made from tantalum have been used successfully in the work on americium, curium, neptunium, and protactinium. All four materials were in the form of the oxide below about 1400°C, and were converted to the carbide above this temperature. The americium research shows that the tantalum is a satisfactory container for the pure metal as well. The work on neptunium indicates that metallic uranium interacts with tantalum at beam temperatures. The same effect was found with metallic plutonium. The problem with the uranium was solved by oxidizing the metal and using a carbon reduction technique. A tungsten oven with tantalum slits, with an inner liner to control creep, was found to be an excellent container for plutonium.

The tungsten oven used in the plutonium research is illustrated in Fig. 6. The hole is covered with tantalum slits made from 3- mil foil that is spot-welded onto the front face of the oven. These slits provide an aperture about 10 mils wide out of which the beam effuses. The tantalum ovens are of smaller design than the tungsten ovens for easier heating. They are mounted on a piece of 40-mil tantalum rod to provide good thermal insulation from the main body of the oven loader.

2. Oven Loader

The design of the oven loader used in the plutonium research was influenced primarily by the need for easy mounting of the oven and the need for quick insertion and withdrawal from the atomic-beam machine with minimum disturbance to the machine vacuum. Figure 7 is a pictorial drawing of the loader used in this research. The tungsten oven containing the material sits on the oven platform. The filament is a 0.010-inch thoriated tungsten wire, which is coated prior to heating with a carbon suspension (Aquadag) to increase electron emission. The application to the oven of several hundred volts gives the beam temperature of 1500°C. Using a mounting which brings the entire bottom surface of the oven into contact with the oven platform requires the application to the oven of about 150 watts to achieve the desired temperature.

When it became apparent in the neptunium research that it would be necessary to achieve temperatures of about 2000°C, the oven loader and the oven were both modified. In particular, the oven platform was replaced by a flat plate held by friction in two slots notched into the high-voltage rods. A 0.040-inch hole drilled in the plate is the mounting for the tantalum rod that supports the oven. A ground plate covers the flat plate in order to increase the collection efficiency of the oven when high voltage is applied. This modified oven loader is illustrated in Fig. 8.

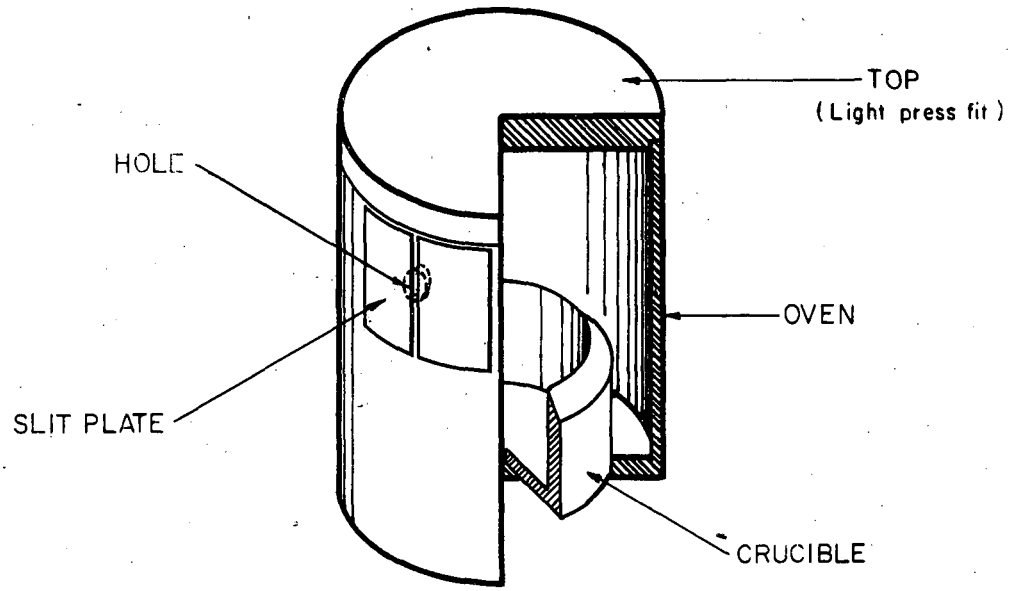

Fig. 6. Cutaway view of oven used for production of a plutonium beam.

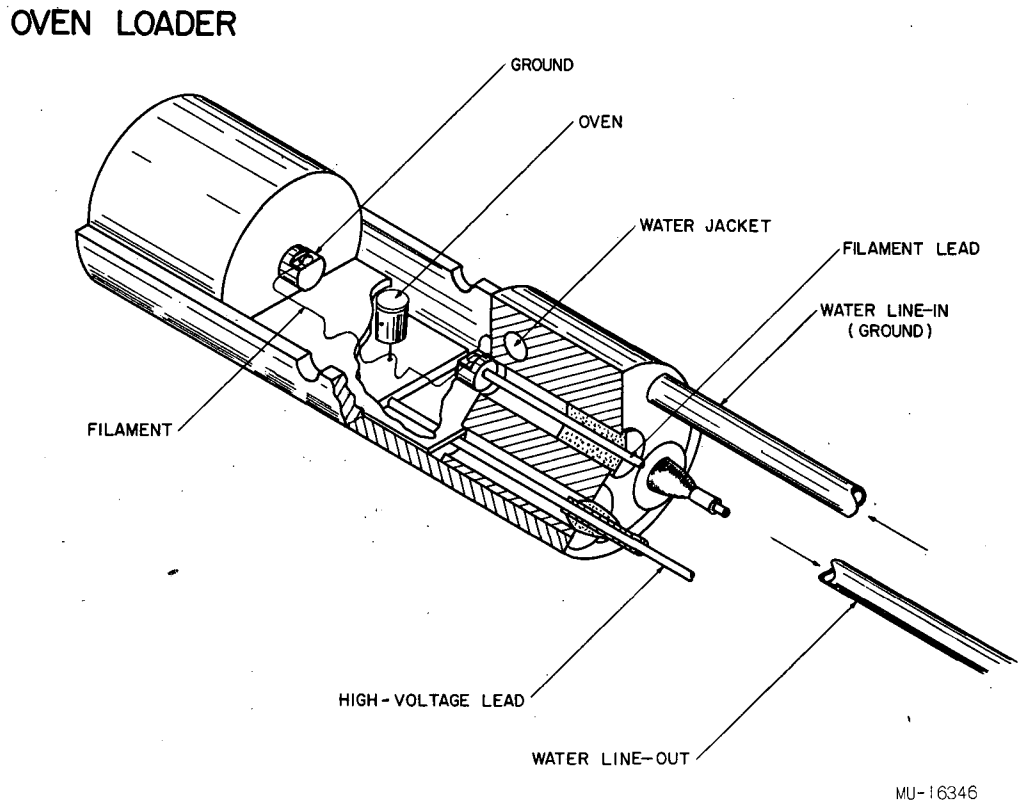

Fig. 8. Modified high-temperature oven loader used in researches at 2000°C.

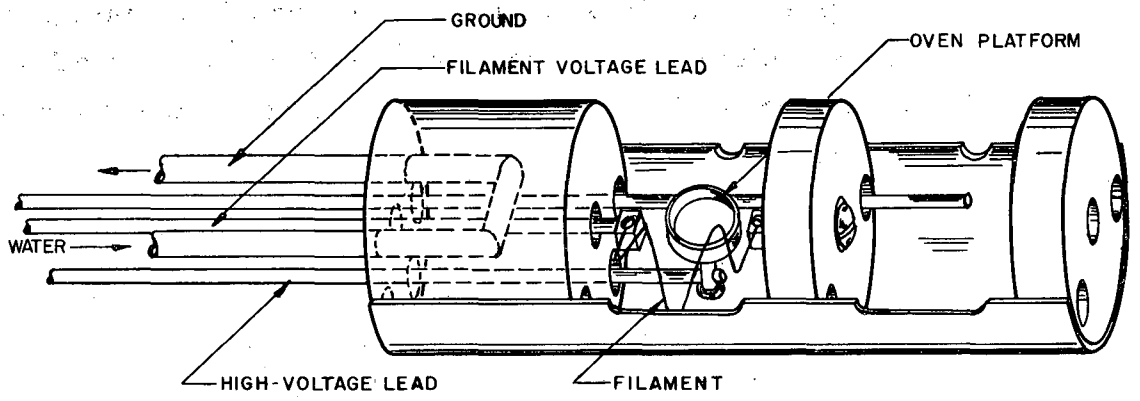

Fig. 7. Oven-loader system for high-temperature electron bombardment used in the plutonium research. The oven (Fig. 6) is placed in the cup and the unit capped with a **matching semicylinder which serves as a heat shield.**

3. Detectors

Thin (0.001-inch) platinum foils have been used successfully as collectors for all elements investigated so far in the transuranic region. These foils have a radius of 0.250 inch and are well adapted to use with the alpha-particle counters and the gas-flow proportional counters used for detection of beta rays. The collection efficiency for the transuranic element beams is high, reproducible, and very probably 100%.

In the earliest runs on Np^{239}, sulfur-coated brass buttons were used as collectors. These buttons are especially adapted to the beta-gamma-ray scintillation counters used in the work on thallium.[30] The efficiency of these detectors for neptunium collection is also high and reproducible.

CURIUM-242

The impetus to the curium research was the availability in solution of curium salts in quantities of hundreds of micrograms. A 2-ml solution containing 100μg of curium, almost entirely 162-day Cm^{242} by activity, was received from Livermore. The substance was identified from its alpha spectrum on the low-background 50-channel UCRL pulse-height analyzer.

Experimental Detail

The chemistry technique involved is to convert the curium salt to the oxide and to reduce the oxide to the metal in the same manner as described in the neptunium research. In detail, the procedure is as follows. From the main body of the solution, 150 microliters is pipetted off and mixed with an excess of concentrated HNO_3. A few mg of uranyl nitrate is added to provide a carrier. The solution is then boiled down on a hot plate to yield a crystalline green material, presumably uranium nitrate. This substance is placed in a platinum crucible which is then heated to a cherry red in an induction heater. This heating is sufficient to decompose the nitrate into the oxide. The quantity of material obtained in this way is in general sufficient to provide 4 to 6 hours of running time at a direct beam rate, with the deflecting magnets off, of about 75 counts per minute incident on the detector.

The conversion in the oven to the carbide takes place at about 1200°C. When the oven temperature is raised to 1800°C decomposition takes place and a beam is formed. This technique for achieving a beam worked in the initial attempt, and no difficulties were ever encountered subsequently.

During the runs the beam was collected on platinum foils. Counting was done in low-background (≈ 0.5-cpm) alpha chambers.

Experimental Observations

A low-field search was made ($\frac{\mu_0 H_0}{h}$ = 0.998 Mc) with the purpose of observing resonances in the frequency region corresponding to g values between 0 and 3.0. Three prominent resonances were observed at frequencies ν_1 = 1.625 Mc, ν_2 = 1.737 Mc, and ν_3 = 1.937 Mc. A fourth resonance in apparently lower intensity was observed at ν_4=2.500 Mc. In order to ascertain more carefully the g values of these resonances, the field was tripled and observations were made at $\frac{\mu_0 H_0}{h}$ = 2.969 Mc (Fig. 9). The transitions were again observed at $\frac{\mu_0 H_0}{h}$ = 9.679 Mc, and finally at a field $\frac{\mu_0 H_0}{h}$ = 18.786 Mc. The resonances at this maximum field (Fig. 10) give the precision values obtained for the g's. The results of the searches are indicated in Table II along with the mean g value for each of the transitions. It is shown in a subsequent section that these g values can very probably be ascribed to electronic states with J = 2, J = 3, J = 4, and J = 5. Hence the corresponding g value is denoted by a subscript.

It was next desired to obtain a measure of the energy-level splitting of the four levels, by observing the relative intensity of each of the four resonances at maximum transition probability. The relative ordering is already crudely indicated by the average intensity of the previously observed resonances to probably be J = 2, J = 3, J = 4, and J = 5, in increasing energy. A more quantitative measure of the splitting is accomplished in the following way. At a low field, the frequency is adjusted for resonance in the state J = 2, and the rf current in the hairpin is varied. The low field minimizes the effect of field fluctuations during an exposure. The adjustability of the rf current is to about 1 ma. For each value of the current, the resonance intensity is obtained (Fig. 11). The current for the maximum of this curve is noted to be about 27 ma, and the current for maximum transition probability in the other J states is obtained by making it inversely proportional to the g value. The theoretical justification for this procedure stems from the Majorana formula, and is discussed in the section on curium energy levels. Observed intensities at maximum are given in Table III.

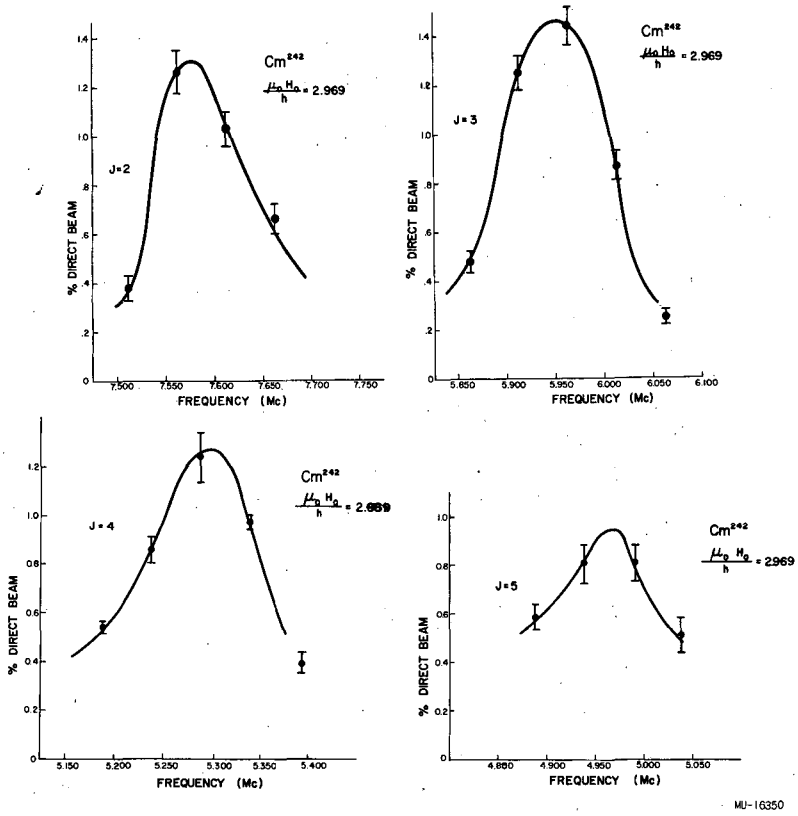

Fig. 9. Observed curium resonances at 2.1 gauss.

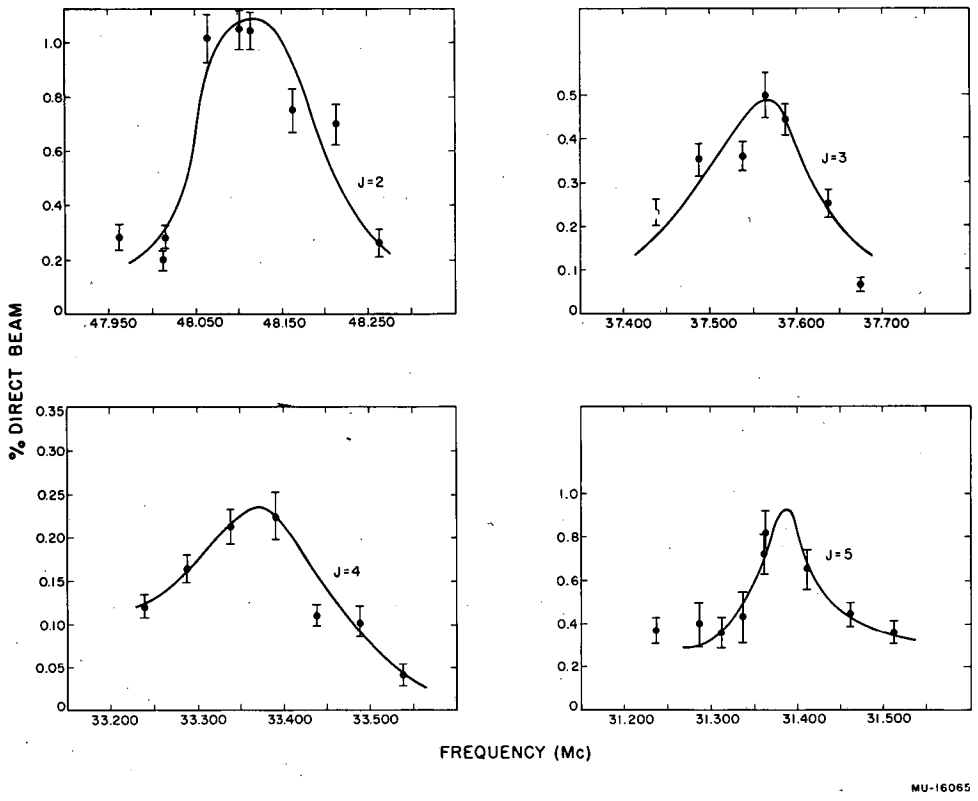

Fig. 10. Observed curium resonances at 13.4 gauss.

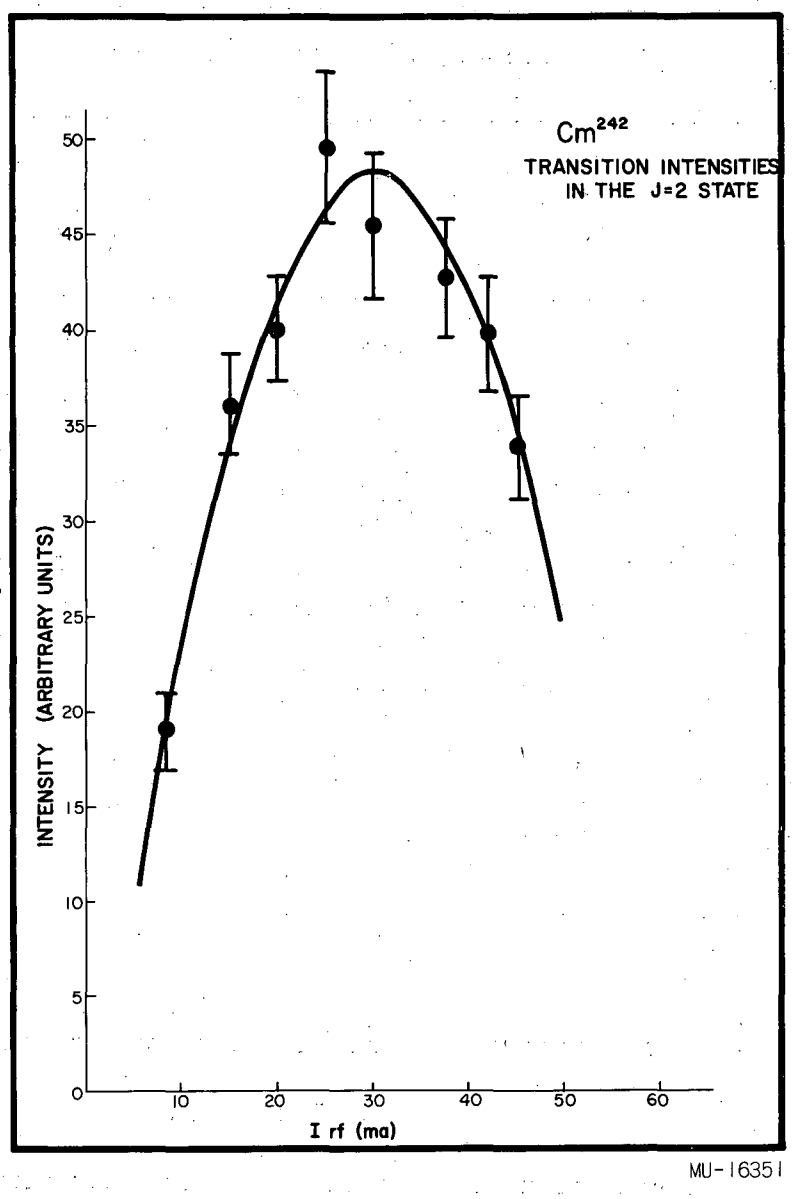

Fig. 11. Variation of resonance intensity in the J = 2 state of Cm^{242} with rf current.

Table II

Summary of experimental observations

$\mu_0 H_0$ / h (Mc.)	$g_J = 2$	$g_J = 3$	$g_J = 4$	$g_J = 5$
0.998	2.50±.05	1.95±.05	1.74±.04	1.63±.04
2.969	2.554±.016	2.00±.02	1.78±.02	1.67±.02
9.679	2.561±.012	2.000±.008	1.772±.009	------
18.786	2.561±.003	2.000±.003	1.776±.002	1.671±.003
Weighted mean	2.561±.003	2.000±.003	1.776±.002	1.671±.003
Calculated values for scheme $J_1=7/2$, $g_{J1}=2.002$; $J_2=3/2$, $g_{J2}=0.890$	2.558	2.002	1.780	1.668

Table III

Resonance intensity in each of the four states at the rf current setting that maximizes the transition probability

State	Observed Intensity (%)
J = 2	1.45±.25
J = 3	1.08±.17
J = 4	0.83±.12
J = 5	0.43±.06

Curium Energy Levels

On the basis of intensity measurements, it is possible to obtain a crude measure of the energy separations of the ground state and first three excited states in curium. As discussed in the section on resonance height, we may write, for the intensity at resonance,

$$I_J = c \exp(-E_J/kT) \sum_{m_J=1}^{J} \overline{P}_J^{\,m_J,-m_J} A_{m_J} . \qquad (V.1)$$

The notation is the same as before. The apparatus factor is included with a subscript, since it depends on the magnetic substate of the atom being flipped. The additional energy imposed on the atom by the external magnetic field is taken as negligible compared with the zero-field energy of the state, hence we neglect it.

In calculating energy separations, only the relative intensities of two transitions are of interest:

$$I_{J_1}/I_{J_2} = \exp\left[(E_{J_2}-E_{J_1})/kT\right] \sum_{m_J}{}' \overline{P}_{J_1}^{\,m_J,-m_J} A_{m_J} / \sum_{m_J} \overline{P}_{J_2}^{\,m_J,-m_J} A_{m_J}$$

$$\text{or } E_{J_2}-E_{J_1} = kT\,\ell n\left(I_{J_1} \sum_{m_J} \overline{P}_{J_2}^{\,m_J,-m_J} A_{m_J} / I_{J_2} \sum_{m_J} \overline{P}_{J_1}^{\,m_J,-m_J} A_{m_J}\right). \qquad (V.2)$$

The flop-in transitions for each J state over which the sum is to be taken are immediately evident from inspection of a hyperfine-structure diagram (Fig. 12). They are:

$J = 5$: $m_J = 5 \leftrightarrow m_J = -5$; $m_J = 4 \leftrightarrow m_J = -4$; $m_J = 3 \leftrightarrow m_J = -3$;
$m_J = 2 \leftrightarrow m_J = -2$; $m_J = 1 \leftrightarrow m_J = -1$.

$J = 4$: $m_J = 4 \leftrightarrow m_J = -4$; $m_J = 3 \leftrightarrow m_J = -3$; $m_J = 2 \leftrightarrow m_J = -2$;
$m_J = 1 \leftrightarrow m_J = -1$.

$J = 3$: $m_J = 3 \leftrightarrow m_J = -3$; $m_J = 2 \leftrightarrow m_J = -2$; $m_J = 1 \leftrightarrow m_J = -1$.

$J = 2$: $m_J = 2 \leftrightarrow m_J = -2$; $m_J = 1 \leftrightarrow m_J = -1$.

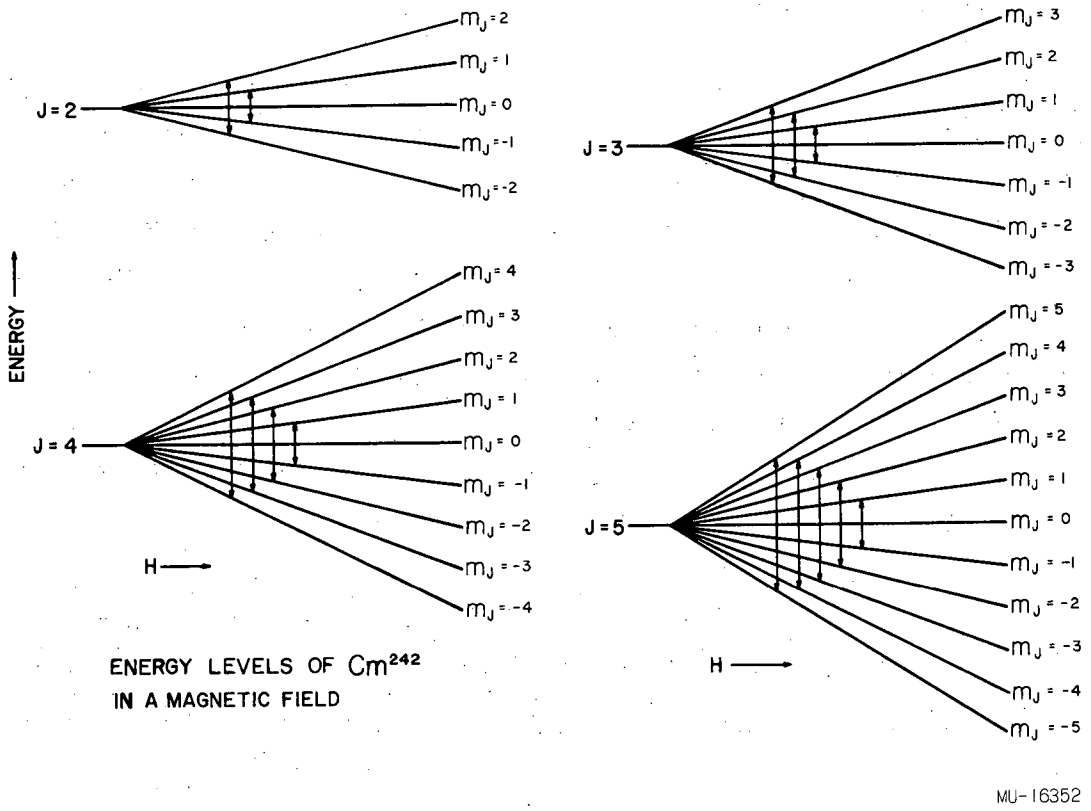

Fig. 12. Energy levels of the four observed J states of Cm^{242} in a magnetic field (not to scale). The arrows indicate the observable transitions.

By use of the empirically determined value of c, the apparatus factor can be calculated for each of these transitions. To within a few per cent, this can be set equal to unity for all transitions.

The calculation of the quantity $\sum_m \overline{P}_J^{m;-m}$ for each of the observed transitions was done on the IBM 650 computer for various values of the parameter $(b/a)^2$. These calculations assume that the system is in the Zeeman region so that all transitions are simultaneously resonant. In this computation, the finite limits of integration were chosen so that the error of neglect was about 1%. The result of the calculation is shown in Fig. 13 as a plot of the quantity $\sum_m \overline{P}_J^{m;-m}$ vs $(b/a)^2$ for each state J. A check on the correctness of the calculation is that in the limit of large $(b/a)^2$, the curves must approach the value (J/2J+1), in good agreement with the calculated probabilities at this limit. It is to be noted that the curves maximize at about the same values of $(b/a)^2$. It is this feature which justifies the technique used for adjusting the rf current as described in the section on experimental observations.

A check on the applicability of the Majorana formula to this work is shown in Fig. 14. Here the experimentally determined resonance-intensity curve for the state J = 2 is plotted to the same scale as the theoretically evaluated transition-probability curve. As was done for the K^{39} data, the scale factor and normalization factor are arbitrary and were chosen to give maximum agreement.

Substituting the observed values for the resonance intensities, calculated transition probabilities, and beam temperature into Formula (V.2) yields the result that the level ordering is normal with the energy separations indicated in Fig. 15.

Electronic Structure

A model for electronic structure in the ground state of curium similar to that which explains the neptunium results can be used to give satisfactory agreement with the observed g values. The assumed ground-state configuration is $5f^7\ 6d\ 7s^2$. The Hund's Rule ground-state term for the configuration $5f^7$ is $^8S_{7/2}$, with a g value $g_J = 2.002$;

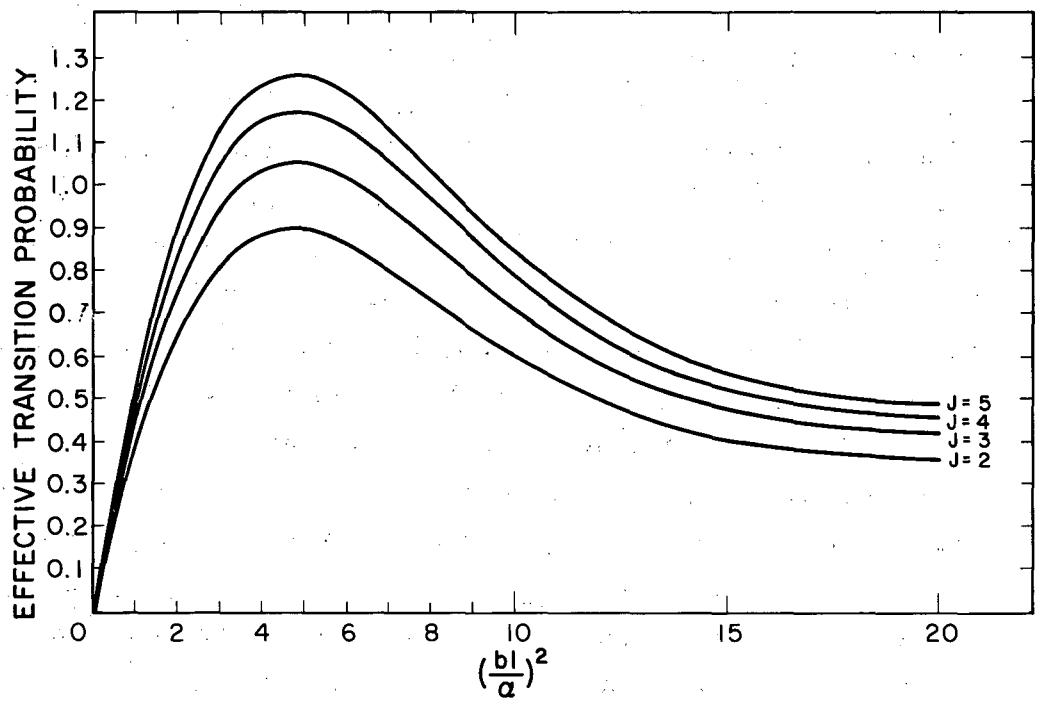

Fig. 13. Calculated transition probabilities for the four states of curium. The abscissa is a quantity which is proportional to the square of the applied rf current. The ordinate is the sum over all flop-in transitions in the particular J state, of the Majorana transition probabilities averaged over the atomic-beam velooity distribution.

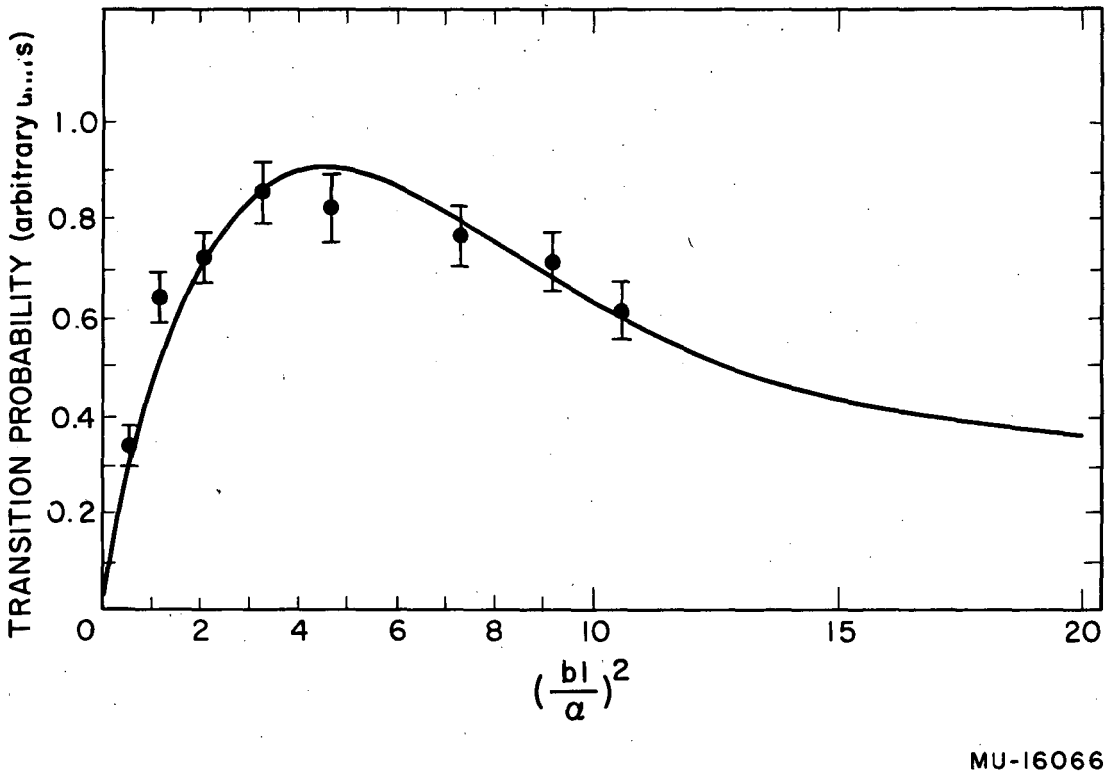

Fig. 14. Comparison of experimental observations and the theoretical transition probability in the J = 2 state of curium.

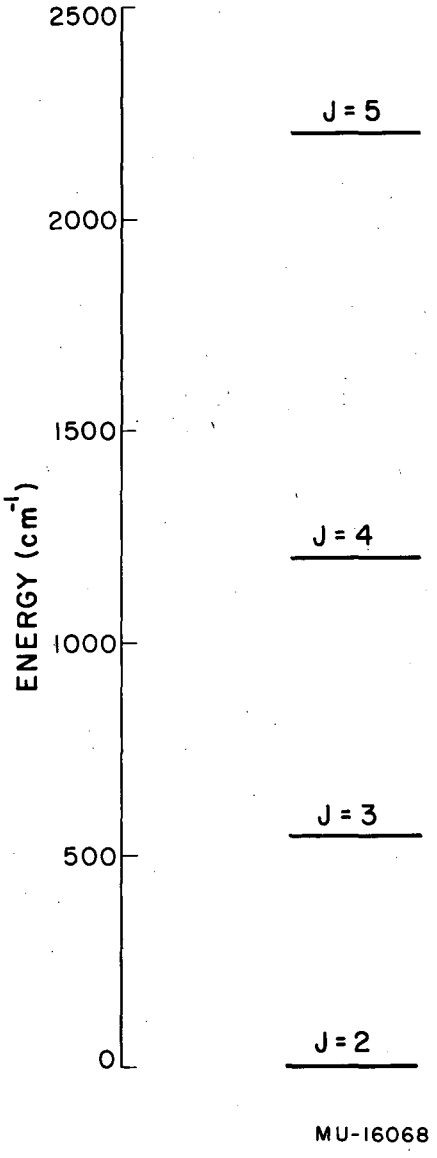

Fig. 15. Approximate curium energy levels as inferred from transition intensities.

for $6d^1$ is $^2D_{3/2}$, with $g_J = 0.800$. Pure j-j coupling between the shells yields a ground-state multiplet consisting of four levels characterized by $J = 2$, $g_J = 2.603$; $J = 3$, $g_J = 2.002$; $J = 4$, $g_J = 1.762$; $J = 5$, $g_J = 1.641$. It is seen that good agreement is obtained in all cases; the largest deviation occurs in the $J = 2$ state and is equal to 2.3%. A model giving agreement with all the observed g values is one in which the $^2D_{3/2}$ state is slightly perturbed so that the 6d electron is described by a state $J = 3/2$, $g_J = 0.890$. In the limit of pure j-j coupling between this state and one characterized by $J = 7/2$, $g_J = 2.002$, the set of g values shown in Table II is obtained. These are compared with the experimental g values.

The rare earth analog to curium is gadolinium, which is found to have a ground-state configuration $4f^7\ 5d\ 6s^2$. Optical spectroscopic measurements of the energy levels indicate that they are fitted very well in the limit of pure L-S coupling.[31] Considering the configuration $5f^7 6d$ in L-S coupling, one finds that it yields a ground-state term ^9D, which gives rise to levels $J = 2$, $g_J = 2.668$; $J = 3$, $g_J = 2.083$; $J = 4$, $g_J = 1.850$; $J = 5$, $g_J = 1.733$; and $J = 6$, $g_J = 1.667$. The configuration $5f^8\ 7s^2$ in the limit of pure L-S coupling leads to a term ^7F, with J values from 0 to 6, all having $g_J = 1.50$. It is clear that none of these latter possibilities is in good agreement with the data.

Nuclear Spin

Implicit in the above discussion of electronic structure is the assumption $I = 0$. Further, no integer values of I and J can fit the observed g values if the system is assumed to be in the Zeeman region of hyperfine structure.

PLUTONIUM-239

Introduction

Prior to the atomic-beam work described here, plutonium had been investigated with respect to its electronic and nuclear properties by the methods of optical spectroscopy and paramagnetic resonance. Van Den Berg, Klinkenberg, and Regnaut[32] first observed the optical spectrum and found the nuclear spin to be 1/2. The observations of Bleaney and co-workers[33] on the paramagnetic resonance spectrum of Pu^{239} verified the spin assignment. In addition, they were able to estimate the nuclear magnetic moment to be about 0.4 nuclear magneton. These measurements indicated that the ground-state electronic configuration of plutonium ought to be either $5f^5\ 6d\ 7s^2$ or $5f^6\ 7s^2$, with a preference for the latter.

The purpose of the measurements to be described herein was to establish the ground-state configuration so far as is possible from a measurement of the g_J and J values of the electronic ground state. In addition, it was desired to measure the hyperfine-structure separation so that a calculation of the nuclear magnetic moment could be made. Finally, as a secondary purpose, a verification of the spin of Pu^{239} was desired.

Hyperfine Structure

Since the spin of Pu^{239} is known to be 1/2, the highest-order nuclear moment possible is a magnetic dipole moment, so that the interaction Hamiltonian is of the form

$$\mathcal{H} = ha\,\vec{I}\cdot\vec{J} - g_J\mu_0\vec{J}\cdot\vec{H}_0 - g_I\mu_0\vec{I}\cdot\vec{H}_0 \,. \qquad \text{(VI.1)}$$

This Hamiltonian is identical to (II.3), which leads to the Breit-Rabi equation and which applies to the case $J = 1/2$. Hence, the energy levels of plutonium can be obtained by interchange of I with J and g_I with g_J in the Breit-Rabi equation, Eq. (II.4),

$$W = -\frac{\Delta W}{2(2J+1)} - g_J\mu_0 m_f H_0 \pm \frac{\Delta W}{2}\left[1 + \frac{4m_f x}{2J+1} + x^2\right]^{1/2} ;$$
$$x = \frac{(g_J - g_I)\mu_0 H_0}{\Delta W} \quad ; \quad \Delta W = ha\,\frac{2J+1}{2} \,. \qquad \text{(VI.2)}$$

For the case J = 1, the electronic state primarily observed, the energy levels are plotted as a function of field in Fig. 16.

It is of interest to note that if the possibility of multiple quantum transitions is excluded, then there are no flop-in transitions present. The possible multiple quantum transitions are $F = 3/2$, $m_f = 1/2 \leftrightarrow m_f = -3/2$ and $F = 3/2$, $m_f = 3/2 \leftrightarrow m_f = -3/2$.

Experimental Detail

The relatively long half life of Pu^{239} (24,000 years) necessitates the use of quantities of the order of milligrams in any given run. Plutonium metal was obtained in foil form approximately 0.005 inch thick and in suitable quantity by weight. This foil was established to contain measurable quantities of Pu^{240} and Pu^{242} by activity.

For use during a run, approximately 50 mg was cut from the foil in the form of small strips and placed in a small tungsten crucible which serves as an inner liner for the tungsten ovens used in this work (Fig. 6). The necessity for an inner liner results from the fact that at beam temperatures, the plutonium melt creeps along the walls of the tungsten oven and attacks the tantalum slits used to define the beam aperture. It is found that the sharp lip on the edge of the crucible serves to prevent creep. With these ovens, beams lasting for 15 hours were obtained with no sign of interaction observed at the beam temperature of about 1500°C.

The characteristic alpha-particle radiation from Pu^{239} serves as a convenient means for the detection and identification of the material. Observation of the alpha spectrum on the 50-channel UCRL alpha analyzer served to establish the composition of the deposit on the plutonium foil, and on the resonance buttons taken during runs. Counting of the buttons exposed during runs was done in 2π alpha counters with backgrounds of 0.10 counts per minute except for occasional bursts due to line noise. Typical counting rates for resonance peaks were 1 or 2 cpm. Countdowns of several hours were taken for each button, and were repeated at least three times so as to eliminate the possibility of a high counting rate due to the indicated line noise.

It was believed at the start of the experiment that a change in the usual method of running would be necessitated by the fact that the states are of integral J only. As noted in the section on hyperfine structure, no single-quantum flop-in transition exists for such a system. A solution to the problem is to use an off-center oven geometry wherein the oven slits are placed about 0.020 inch off an axis down the center of the magnet gap. Such a geometry permits a refocusing of transitions in which an atom goes from the state $m_I, m_J = 0$ in the A magnet to either one of the states $m_I, m_J = +1$ or $m_I, m_J = -1$ in the B magnet, depending on which side of the axis the oven is placed. Figure 17 shows the off-center geometry and the trajectory of an atom undergoing such a transition. This oven geometry was used throughout most of this work. As is described in the next section, however, the apparent existence of very intense multiple quantum transitions in the intermediate-field region made the off-center geometry unnecessary.

Experimental Observations and Data

An initial search for resonances taken with a C field of 0.7 gauss ($\frac{\mu_0 H_0}{h}$ = 0.996 Mc) was made with the off-center oven geometry to obtain information regarding the electronic ground state of plutonium. Resonances were found at frequencies corresponding to g values of 1.0, 1.2, 1.5, and 1.8 (Fig. 18). The resonance at 1.0 was tentatively ascribed to the system $g_J = 3/2$, $J = 1$, $I = 1/2$. Since the sample is known to contain 5% to 10% Pu^{240} by activity, the resonance at 1.5 Mc is probably due to a system with the same electronic state and $I = 0$.

In order to improve the precision and reliability of these low-field data, the strongest observed transition--that corresponding to $g_f = 1$ and presumed to arise from the $J = 1$ first excited state and the $F = 3/2$ level--was followed to a higher field. Further observation of the $F = 3/2$ state at 1.4 gauss ($\frac{\mu_0 H_0}{h}$ = 1.985 Mc) showed the observed resonance to deviate by about 0.150 Mc from the resonant frequency predicted on the assumption that the system is in the Zeeman region (Fig. 19). This deviation is referred to as the quadratic shift, since it is a good

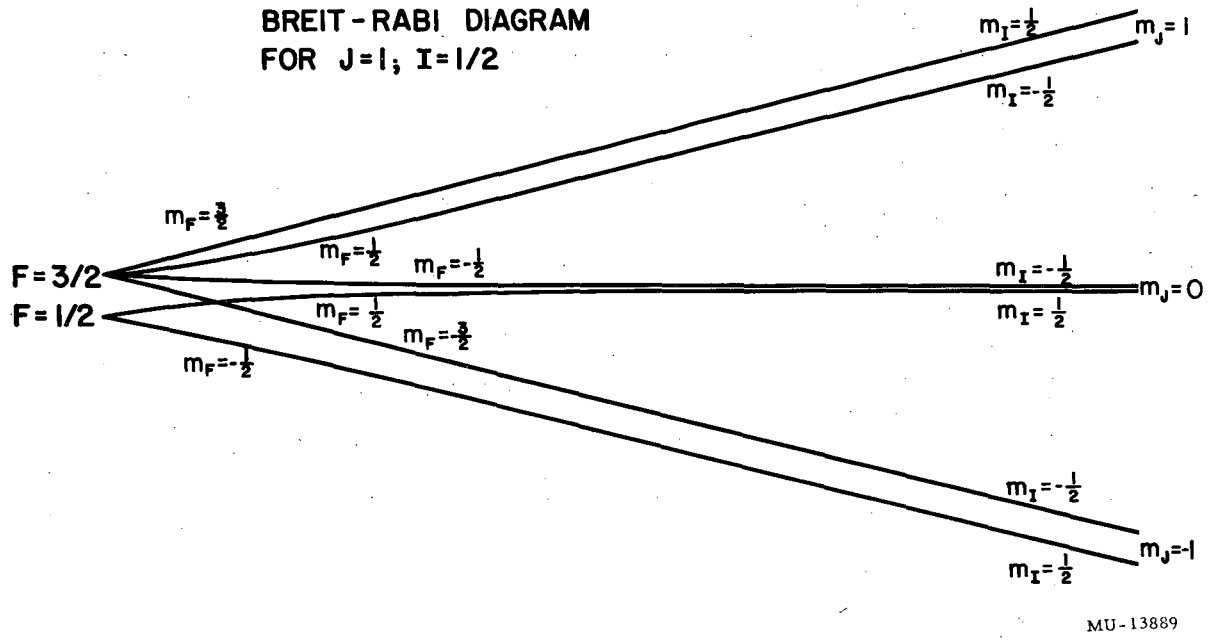

Fig. 16. Energy levels of the system J = 1, I = 1/2 in a magnetic field.

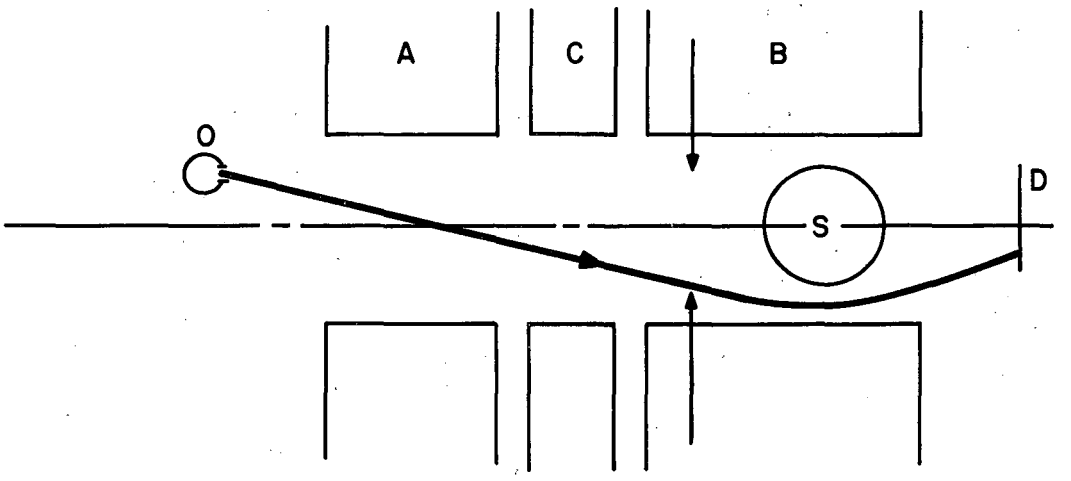

FLOP-IN TRAJECTORY
WITH OFF-CENTER
OVEN GEOMETRY

MU-16353

Fig. 17. Hypothesized flop-in trajectory of an atom undergoing the transition $\Delta F = 0$, $\Delta m = \pm 1$ in a state of integral J using the off-center oven geometry.

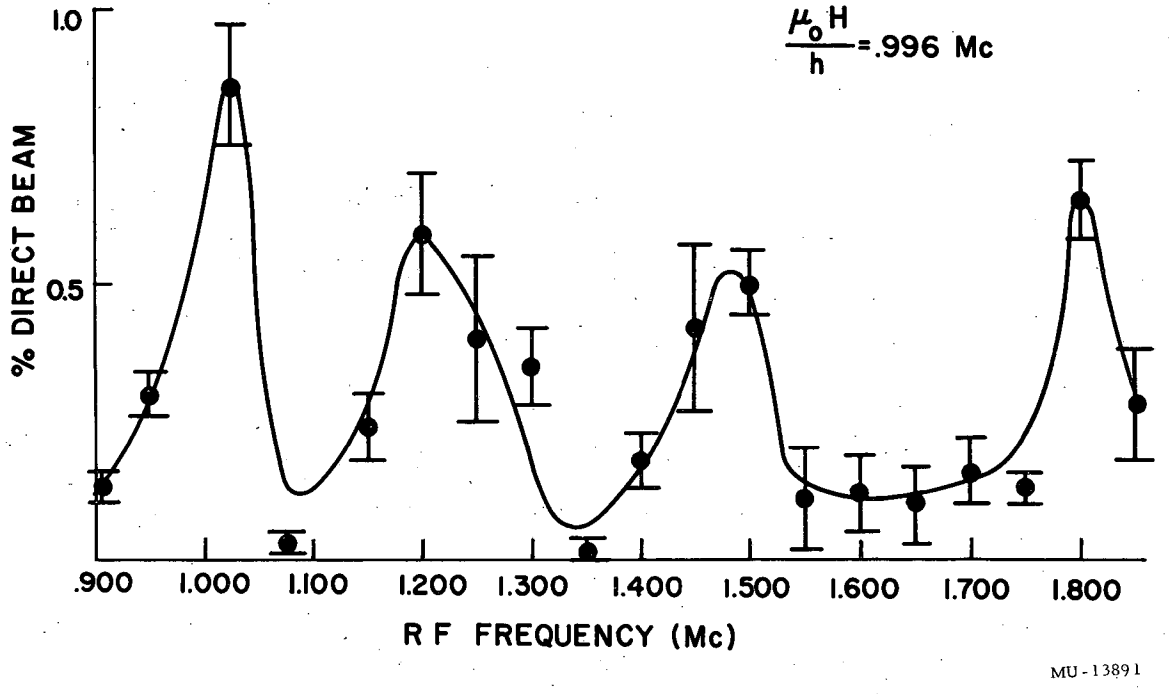

Fig. 18. Results of a very-low-field search to obtain information regarding the electronic ground state of plutonium.

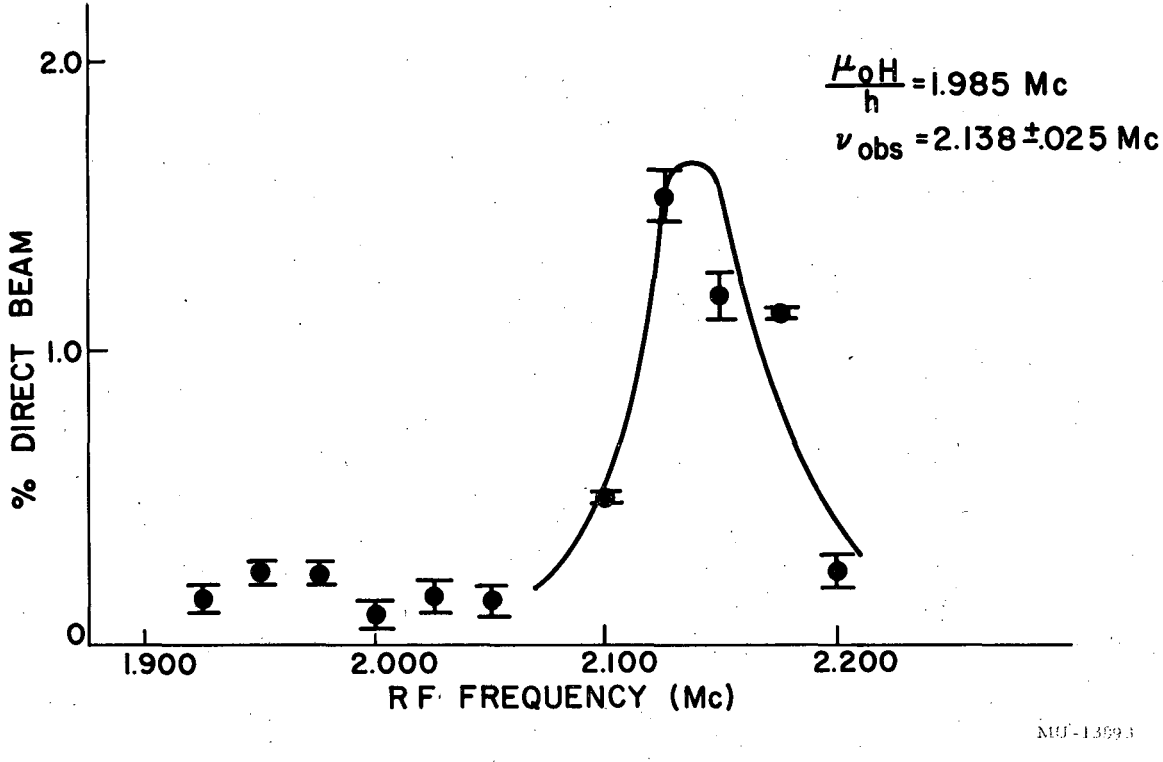

Fig. 19. Observed plutonium resonance at 1.4 gauss.

approximation to assume that it arises from a term quadratic in the field. Its large value at this low field is characteristic of an extremely small hyperfine structure.

Since the hyperfine-structure separations are expected to be about the same in all states arising from the ^7F multiplet, and since $J = 2$ and $J = 3$ state contamination are known to be strongly present in the beam, the complexity of intermediate-field structure is considerable. Hence improvement in the value of ΔW was obtained by following the transition through intermediate field in small increments in the field. All resonances taken in this region are displayed in Fig. 20 along with those observed later at fields in the Paschen-Back region of hyperfine structure.

A reasonably precise estimate of ΔW was obtained by using the procedure just described and the Formula (VI.2) for the energy levels. An attempt was then made to observe the transition $\Delta F = \pm 1$. The transition $F = 3/2$, $m_f = 1/2 \rightarrow F = 1/2$, $m_f = -1/2$ can be used for this observation and is an ordinary single-quantum transition. Using the off-center oven geometry, a search was performed at a C field of 0.4 gauss ($\frac{\mu_0 H_0}{h} = 0.500$ Mc) yielding an effect at about 8.5 Mc which was ascribed to the desired transition and which was later traced out in detail (Fig. 21). The hyperfine structure yielded by these resonances is the assigned value of $7.683 \pm .060$ Mc. There is also an effect present at 7.7 Mc which is probably due to transitions normally forbidden by apparatus-selection rules but is allowed in first order by the off-center geometry used in this search.

A precise measure of the g_J value by means of a search in the limit of high C field (Paschen-Back region) was made. As described in the theory of experiment, the slope of a straight-line fit to the curve of frequency vs magnetic field taken in this region gives a relatively accurate value of g_J. Moreover, a crude value of the hyperfine structure is obtainable from the frequency intercept of this line.

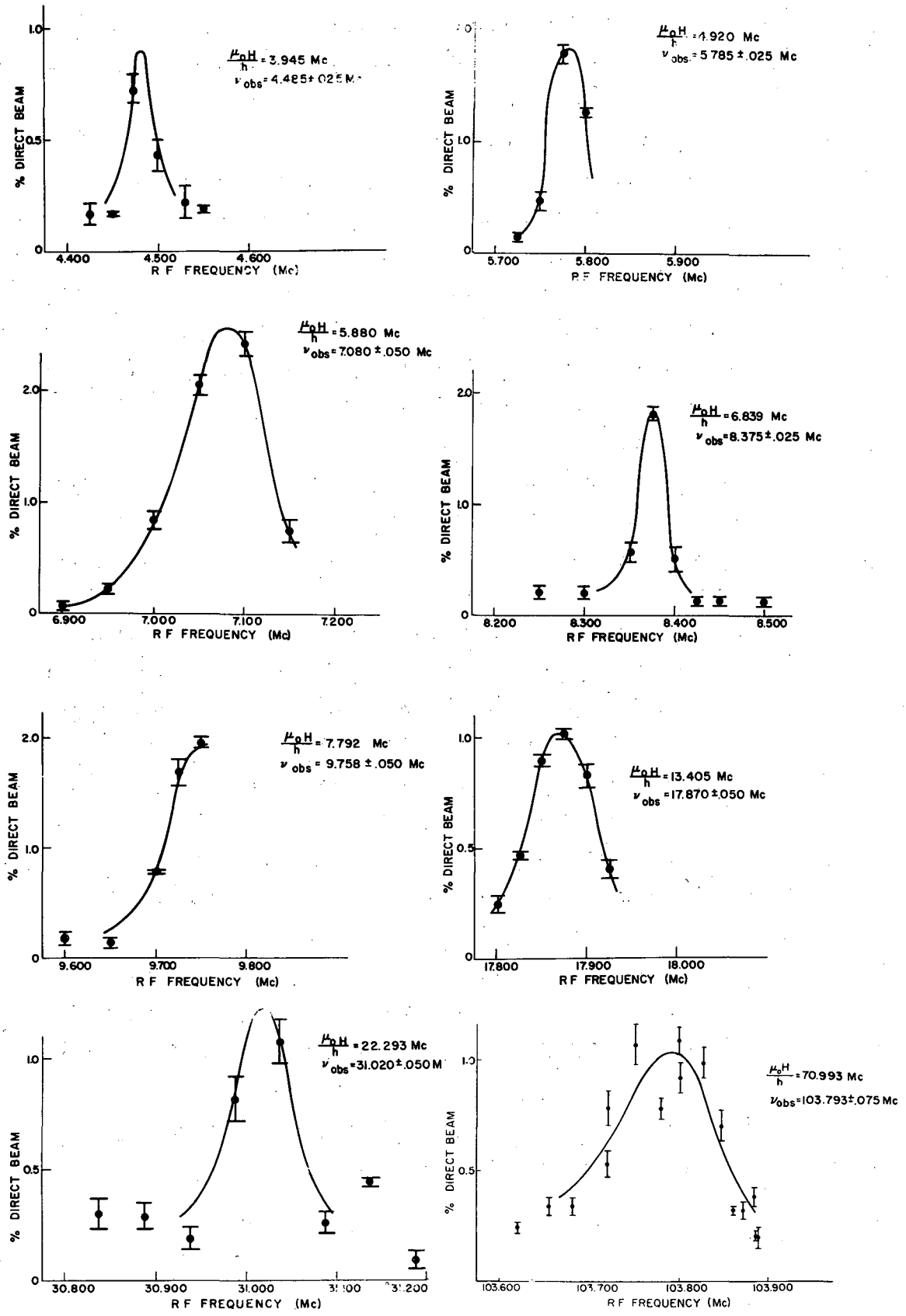

MUB-152

Fig. 20. Observations of the J = 1, F = 3/2, $m_f = 1/2 \longleftrightarrow m_f = -3/2$ double quantum transition in intermediate and strong fields.

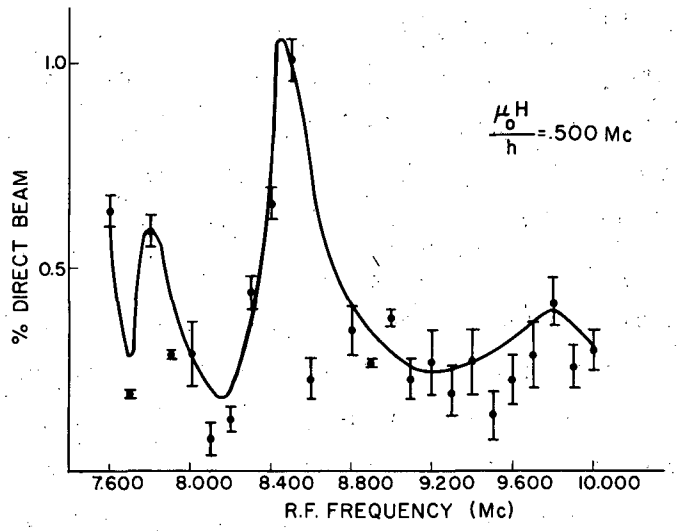

50,198-

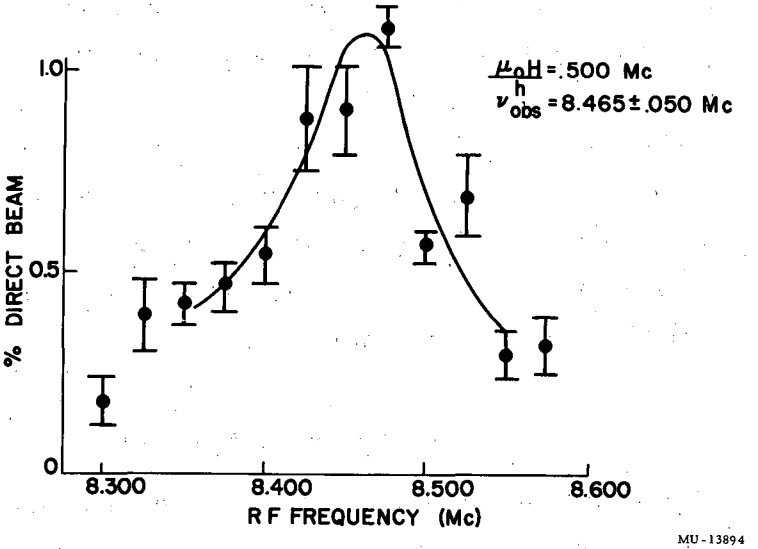

MU-13894

Fig. 21. (a) Data obtained during the search for $\Delta F = \pm 1$ transitions at low field. The resonance near 8.5 Mc is due to the transition $F = 3/2,\ m_f = 1/2 \longleftrightarrow F = 1/2,\ m_f = -1/2$.
(b) Detail of the transition $F = 3/2,\ m_f = 1/2 \longleftrightarrow F = 1/2,\ m_f = -1/2$ on which the hyperfine-structure assignment is based.

A two-parameter fit to all data taken on the $F = 3/2$ transition was attempted under the assumption that the transition under observation was the single-quantum one $F = 3/2$, $m_f = -1/2 \leftrightarrow F = 3/2$, $m_f = -3/2$. No such fit could be made giving agreement with the experimentally observed resonant frequencies to within several mean deviations of all the points. It was found necessary instead to fit the data to the double-quantum transition $F = 3/2$, $m_f = 1/2 \leftrightarrow F = 3/2$, $m_f = -3/2$. The assumption that the observed transition was the double-quantum one was checked experimentally by repeating some of the intermediate field points using an on-center geometry. Such a geometry highly discriminates against a single-quantum transition; however, there was no apparent loss in intensity. On the assumption of a double-quantum transition, and by use of the value of ΔW obtained from observation of the direct transition, a value of g_J was chosen which minimized the root-mean-square error in the experimentally observed points. This yields $g_J = 1.4975 \pm .0010$.

A summary of the result of this fit is shown in Fig. 22, where the difference between the experimental and calculated frequencies is plotted vs $(\frac{\mu_0 H_0}{h})^{1/2}$. This arbitrary abscissa is convenient for the display of the data. The agreement seems to indicate that the errors assigned to the experimental points are rather conservative. The assignments were made by using the adjustability of the C field, which is taken as 15 kc as a lower limit. The upper limit is determined from visual observation of the resonances.

Nuclear Magnetic Moment

Information about the nuclear magnetic moment may be extracted from the measured hyperfine-structure interaction constant, provided an evaluation of the magnetic field at the nucleus can be made. For a system of equivalent electrons such as that found in plutonium, this is in general complicated by the fact that the electronic state may be a mixture of several configurations or that the coupling scheme is intermediate between pure L-S and pure j-j. The observed g_J value of plutonium indicates, however, that the assumption of pure L-S coupling to the Hund's Rule ground state between electrons of the single configuration $5f^6$ is a good one, and we may therefore apply Formula (II.12) to this situation. For

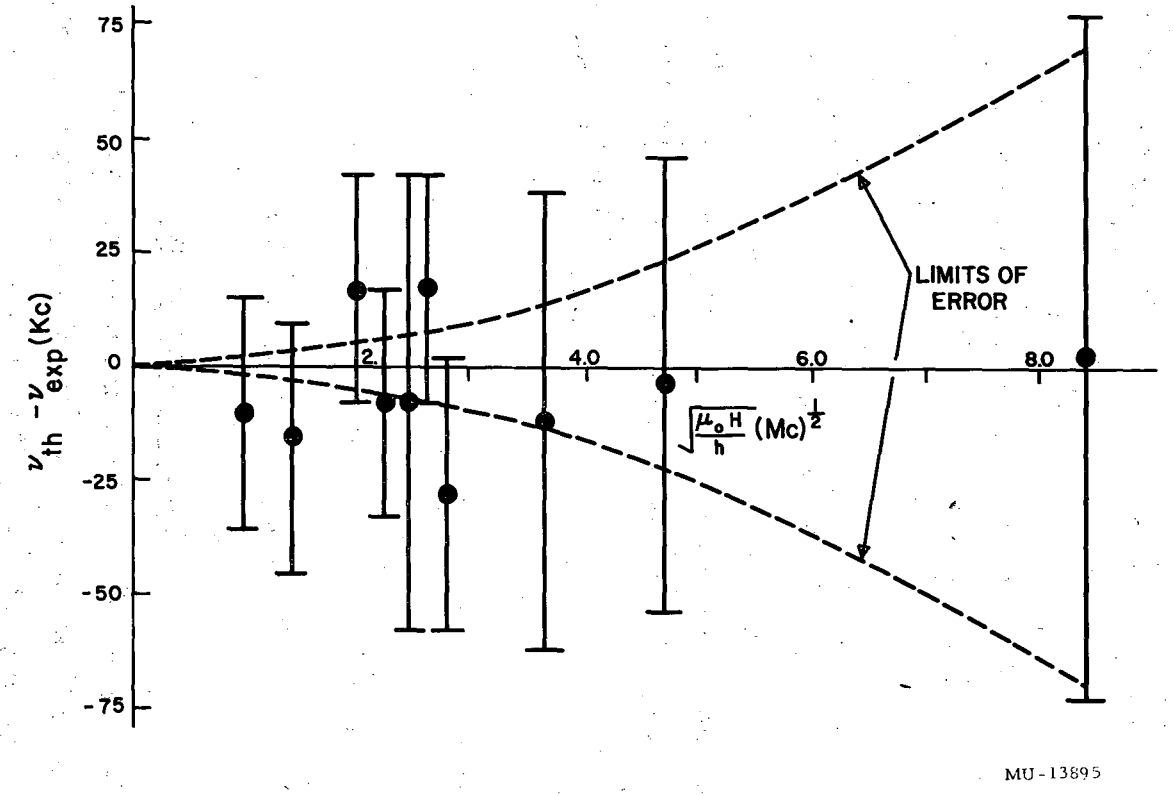

Fig. 22. Summary of all resonance data on the F = 3/2 double-quantum transition. The dotted lines show the permissible range of observations for the given uncertainty in g_J only.

the ^7F_J level this yields

$$a(^7F_J) = g_I\mu_0^2 \left\langle \frac{1}{r^3} \right\rangle \left\{ \frac{J(J+1)+58}{90} \right\} \qquad \text{(VI.3)}$$

and

$$a(^7F_1) = \frac{2}{3} g_I \mu_0^2 \left\langle \frac{1}{r^3} \right\rangle .$$

The value of $\left\langle \frac{1}{r^3} \right\rangle$ appropriate to 5f electrons is estimated from relativistic wave functions calculated for uranium using a Hartree method.[34] This yields:

$$\left\langle \frac{1}{r^3} \right\rangle_{5f} = \frac{1}{2aa_0} \int \frac{FG}{r^2} \, dr = 3.89 \, a_0^{-3}, \qquad \text{(VI.4)}$$

$$\left\langle \frac{1}{r^3} \right\rangle_{5f} = \int \frac{F^2 + G^2}{r^3} \, dr = 3.99 \, a_0^{-3} .$$

The ratio of these two is the relativistic correction factor,[35] which is neglected in this approximation. The value of a is given by

$$a\,(^7F_1) = 2/3 \; g_I \mu_0^2 \; \frac{3.89}{a_0^3} = 124 g_I \text{ Mc.} \qquad \text{(VI.5)}$$

The experimental value

$$a = 2\Delta W/3 = 5.14 \text{ Mc.}$$

Therefore,

$$\mu = g_I \mu_0 I = 2.1 \times 10^{-2} \text{ nm.}$$

Electronic Structure

The observations made in the low-field search (Fig. 18) and on the g_J value of the state J = 1 indicate that the ground-state configuration is almost certainly $5f^6\,7s^2$. The Hund's Rule ground-state term for such a configuration is ^7F coupling to a ground state J = 0 and excited states J = 1, 2, . . . 6. On the assumption of pure L-S coupling, the g_J value of the ground-state term including the effect of the anamolous electron moment is

$$\frac{g_L + g_S}{2} = 1.5012,$$

in good agreement with the experimentally observed g factor. Possible sources of the discrepancy between the theoretical and experimental values are

1. An admixture of j-j coupling between 5f electrons.
2. Higher-order relativistic effects.[19]
3. Diamagnetic shielding.[36]

The results of the low-field search indicate resonances at frequencies corresponding to values of $g_f = 1.2$ and $g_f = 1.8$. This is in approximate agreement with the g values expected from the coupling of the state $J = 2$ with $I = 1/2$. That these resonances are present in about the same intensity adds support to the assumption that they arise from transitions corresponding to the same J state.

The presence in the beam of more than one J state is consistent with the optical spectroscopic measurements by Conway,[37] who has observed a fine-structure splitting constant for Am^{+++} in $LaCl_3$ in the ^7F term of 450 $cm.^{-1}$ When this is used as the splitting constant for 5f electrons, the energy-level diagram of Fig. 23 is applicable with the indicated relative populations of the substates. These are consistent with the resonance intensities observed in the low-field search.

Nuclear Structure

From the measurements made in this experiment, it has been possible to obtain values for I and μ. In addition, the beta decay of Np^{239} and the alpha decay of Cm^{243} have been observed,[38,39] and have yielded a set of six energy levels in the ground-state rotational multiplet of Pu^{239}. These levels and their assigned spins and parities are shown in Fig. 24. The accumulated data can be used to make an analysis of the applicability of the Nilsson model to this nuclide.

The energy-level scheme can be very well fitted to the two-parameter equation (I.1). Such a fit yields, for the value of the decoupling constant, $d = -0.57$, and for the core moment of inertia, $\mathcal{J} = 5.6 \times 10^{-50}$ g-$cm.^2$

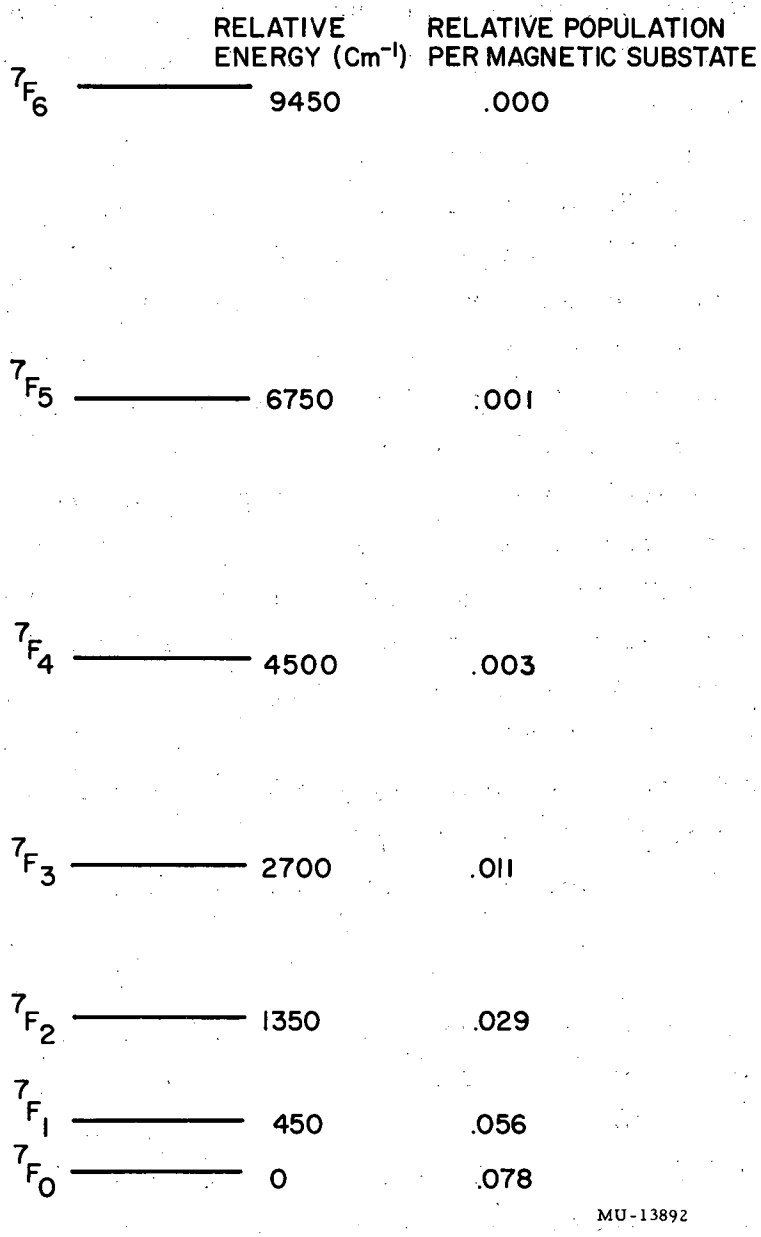

Fig. 23. Approximate ^7F level structure in Pu^{239} inferred from optical spectroscopic data. The relative population per magnetic substate is calculated for 1700°C, the approximate plutonium beam temperature.

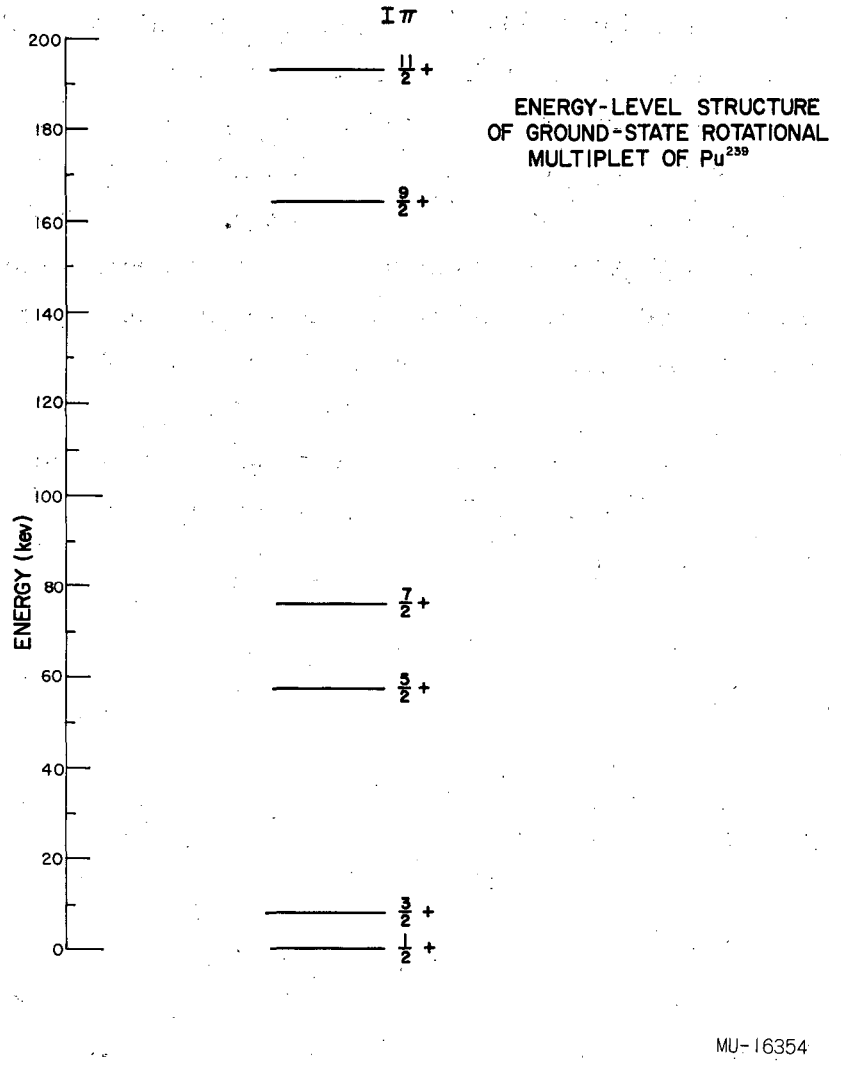

Fig. 24. Observed energy levels in the nuclear ground-state rotational multiplet of Pu^{239}.

The implication of this fit is that the last neutron lies in a level $\Omega = 1/2$. Further, the measured spin of 1/2 is consistent with the empirical decoupling constant. The 1/2+ level in which the last neutron lies can be determined from the calculated set of energy levels published by Nilsson.[7] There is only one 1/2+ level, that which is characterized in the strong-coupling limit by (631+)1/2, which can contain the 145th neutron. Moreover, it can do so only if the deformation parameter of the nuclear core lies within the range of values $2.2 \lesssim \eta \lesssim 2.7$. A calculation of η from the measured decoupling constant is possible if we use the Nilsson wave functions for the indicated state to yield values of d as a function of η. It is unfortunate that over the critical range of the deformation parameter this quantity is rather insensitive to the exact value of a (Fig. 25). However, the measured value indicates that η is about 2.3, within the required range.

From this value of η the magnetic moment is computable, i.e., the matrix elements of Eq. (I.5) can be evaluated. This procedure yields a value of 0.7 nm.

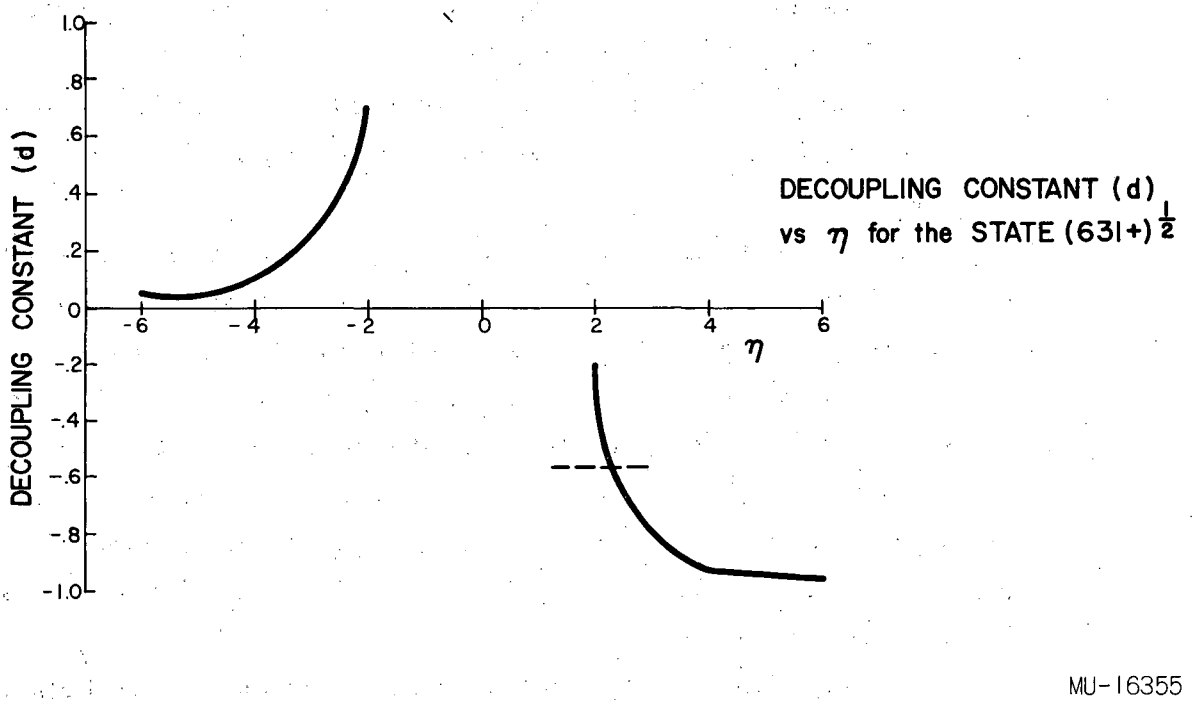

Fig. 25. Variation of the decoupling constant (d) with the deformation parameter (η) for the state (631+)1/2.

NEPTUNIUM-239

Introduction

Prior to the atomic-beam work on this isotope, several investigations bearing on the nuclear spin had been carried out by other groups. Conway and McLaughlin,[40] using the method of optical spectroscopy, had assigned to the ground state a spin of 1/2. This was apparently substantiated by a paramagnetic-resonance experiment.[41] However, a recent re-examination of this paramagnetic-resonance spectrum has indicated a gamma-ray anisotropy in the decay of Np^{239} nuclei aligned in crystals by static hyperfine-structure interactions. This proves $I(Np^{239}) > 1/2$.[42] On this basis, the earlier result is believed to stem from resonances observed on the decay product, Pu^{239}, in an unusual oxidation state.

Less direct inferences concerning the spin were obtained from alpha-particle spectroscopy[43] and beta- and gamma-ray spectroscopy.[44] The alpha-decay measurements showed an almost one-to-one correspondence in the decay spectra of Am^{241} and Am^{243}. This indicates equivalence of the level structures of the daughter neptunium isotopes to within experimental measurability. Since the spin of both americium isotopes is known to be 5/2,[45] an assignment to the ground state of Np^{239} agreeing with that of Np^{237} is preferred. The spin of Np^{237} has been measured and found to be 5/2.[46]

The branching ratios and lifetimes in the observed beta decay of Np^{239} are extremely difficult to explain if one assumes a ground-state spin of 1/2.[47] On this basis, and using the indicated similarity in the level structures of Np^{237} and Np^{239}, Hollander has assigned 5/2+ as the ground-state spin and parity of Np^{239}.[44]

Isotope and Beam Production

Production of Np^{239} is via the reaction $U^{238}(n,\beta)Np^{239}$, which proceeds with a cross section of 2.76 barns.[48] In order to avoid excessive contamination from the fission products of U^{235}, it is necessary to use a U^{235}-depleted target. The metal used for bombardment in these experiments contained less than 0.4% U^{235} by weight. Bombardment of this material took place initially at the MTR in Arco, Idaho and during the last stages of research at the Argonne pile. An integrated flux of 5.2×10^{19} neutrons per cm.^{2} was obtained from the MTR and 5×10^{18} neutrons per cm.^{2} from Argonne. Conditions of shipment were such that at the time of running, the activity of the sample was approximately one curie irrespective of pile location.

The intense radiation from the target material necessitated special precautions in its handling. All chemistry operations were performed in a lead-shielded cave, and manipulators were used wherever possible to avoid exposure to the hands. A photograph of such a cave is shown in Fig. 26. The operation of loading the oven and placing the oven loader into the apparatus was performed manually in the Berkeley box attached to the apparatus. A radiation dosage of approximately 1 mr/sec during the loading operation was typical at the hands, and a whole-body dosage rate of 1 mr/min was common.

The initial attempt to form a beam was by directly vaporizing the neptunium from the uranium in a tungsten oven covered with tantalum slits. To this end, the target uranium was cut in small slivers, several of which were placed in a tungsten oven. At the operating temperature of 1500°C a steady beam could be obtained in this way for approximately 20 minutes. Breakdown in the operating conditions at the end of this time was signaled by an increase in the machine background of a factor of about ten. Attempts to run despite this increased background showed that it would mask all resonances. At the end of the runs it was found that the oven slits had melted so that the entire slit hole was exposed and that the slit material was apparently spread over the front face of the oven. This was ascribed to molten uranium creeping over the walls of the oven

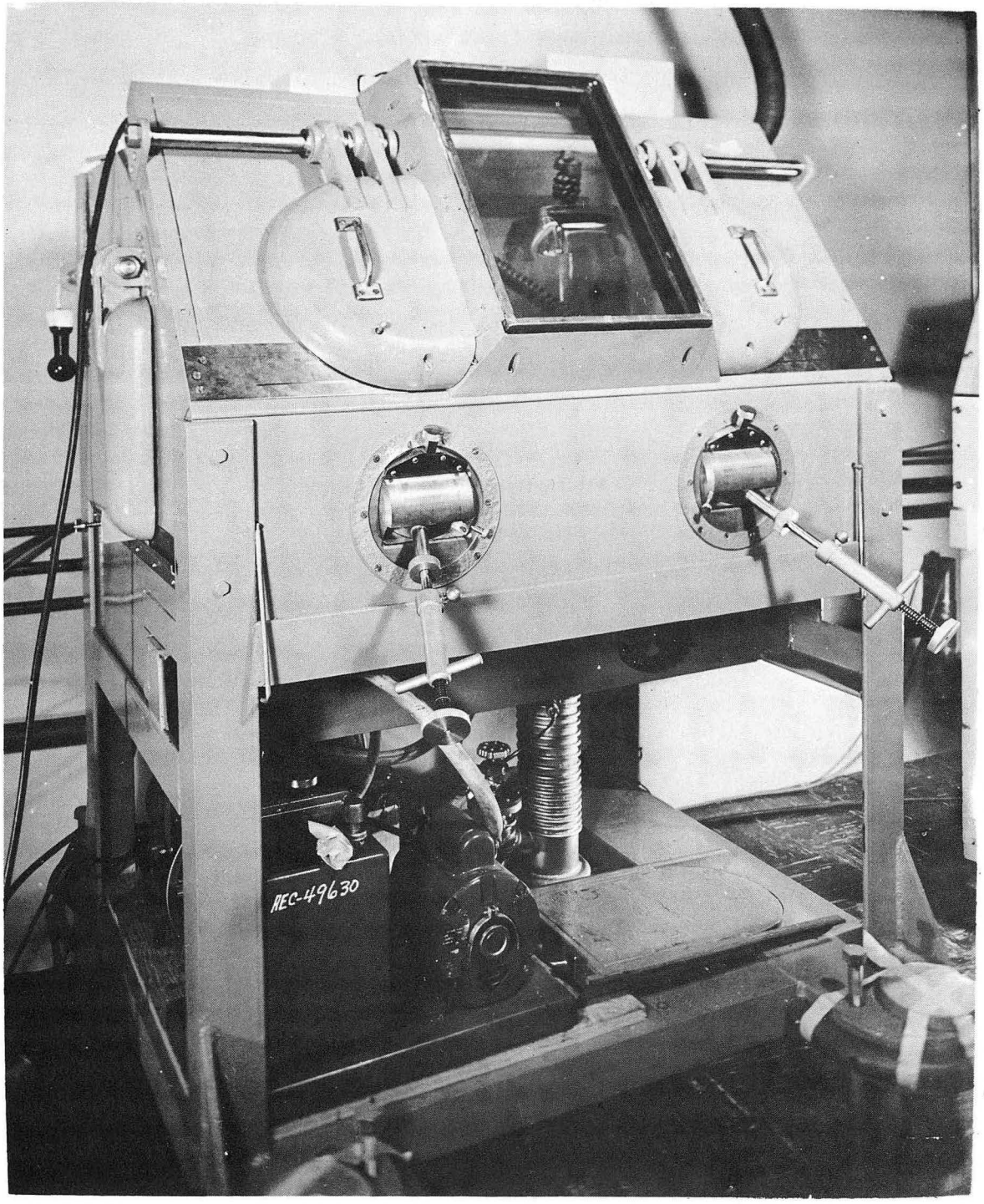

ZN-1662

Fig. 26. Chemistry box of the type used for the neptunium chemistry.

and interacting with the tantalum slits so as to form a low-melting-point alloy. Attempts to control this creep with an inner liner as in the plutonium research failed.

As direct vaporization was considered hopeless, a chemistry procedure was then attempted. The result of the chemistry was to separate the neptunium from the uranium as the fluoride. The resultant neptunium compound was then placed in the oven along with a piece of barium metal. At temperatures of about 1200°C, the barium is supposed to reduce the fluoride to leave neptunium metal. This method failed, apparently because it was impossible to achieve a satisfactory equilibrium in the oven at this temperature. The barium effused out the oven slits at this temperature within 30 seconds. At lower temperatures the reduction would not go at all, and this particular chemistry was abandoned.

The attempts to effuse neptunium directly from the uranium indicated that the vapor pressure of neptunium is larger than that of uranium by several orders of magnitude. It was hoped on this basis that the neptunium could be separated from the uranium in an evaporator. Accordingly apparatus similar to that used in the work on thallium[30] was set up. However, when the capsule containing the uranium sample to be tried was broken open, the material ignited, forming a black power characteristic of uranium oxide. An attempt was then made to salvage the material via the mechanism of carbon reduction. In detail, the procedure is to mix the oxide with an excess of carbon in the tantalum container. The material is then heated to 1700°C, at which temperature a beam of neptunium atoms is formed. The heating process is accompanied by considerable outgassing, presumably due to CO formed during the reduction process. The fact that a workable beam occurs at a temperature of about 1700°C indicates that the mechanism probably involves the decomposition in the vapor phase of neptunium carbide, since the observed vapor pressure is not characteristic of neptunium metal.

The success of the carbon-reduction technique meant abandonment of the evaporation method before it was even tried. On some occasions it was found that a beam of molecules rather than atoms was formed.

This was ascribed to incomplete mixing of the oxide with the carbon. However, in general the reduction technique proved adequate.

Experimental Detail

The procedure for most runs became routine after a successful technique for beam production had been achieved. In general, the running temperature ranged from 1700°C to 2000°C. A direct beam of about 300 cpm for a 2-minute exposure of the detector button with the magnets on was considered a runnable beam. Whether this beam was atomic or molecular in nature was determined by the throw-out ratio, i.e., the ratio of the direct beams taken with the magnets off and with the magnets on. An atomic beam has a throw-out ratio of 5/1; a molecular beam has a throw-out ratio of 3/1. Another characteristic of molecules is the large temperature dependence of its vapor pressure, a factor of 10 per 100°C, in contract with a factor of 4 per 100°C characteristic of atoms.

Two different counting schemes were used in the neptunium work. The primary radiation of Np^{239} stems from two β transitions with end-point energies of 435 kev and 310 kev.[49] Initially neptunium atoms were collected on sulfur-coated brass buttons and counted in the scintillation counters. However, there was enough attenuation in the 0.001-inch aluminum foil so that counting in the gas-flow proportional counters yielded an increase in the counting efficiency by a factor of about four. Platinum foils were used in connection with the flow proportional counters. It is possible that part of the increased efficiency stems from platinum's being a more efficient collector of neptunium than sulfur.

Three factors contribute to the identification of the substance under investigation as Np^{239}. The method of production is such as to yield only Np^{239} and the fission products of U^{235}. An aliquot sample of the bombarded material was pulse-height analyzed on the "Penco" to determine its energy spectrum. No measurable fission-product content was detected although the characteristic β^- spectrum of Np^{239}

was observed. Finally, typical direct-beam and resonance buttons were decayed so as to yield a half-life determination of the material (Fig. 27). The measured half life is consistent with the known half life of 2.35 days.[50]

Experimental Observations and Data

A search for resonances at low field ($\frac{\mu_0 H_0}{h}$ = 2.969 Mc) yielded the results shown in Fig. 28. The relatively broad resonance at 1.4 Mc is explained by assuming two unresolved transitions near this frequency. If one attempts to ascribe these resonances to a single I and J, then the possibility of spin 1/2 is precluded. Further, the pattern is very indicative of the hyperfine-structure system J = 11/2, I = 5/2 although the accuracy of the g values is too low to convincingly establish this assignment. For this reason each of the observed transitions was followed to a C field of 25 gauss ($\frac{\mu_0 H_0}{h}$ = 35.535 Mc). A tabulation of all resonances observed is given in Table IV in terms of the g values assigned to the transitions along with the experimental error. These data were treated in the following way. A mean g_f value was determined from the group of g_f values corresponding to the same transition at different fields. So far as possible, it was desired to make a g_J-independent fit to the data which would yield values of I and J. This was done by considering ratios of g_f values. The g_f value is given by Eq. (II.6) and is given to a good approximation by

$$g_f = g_J \frac{F(F+1) + J(J+1) - I(I+1)}{2F(F+1)} \equiv g_J C_F ,$$

where a term of the order of the nuclear magnetic moment is neglected. If any pair of g_f values belongs to the same J value then their ratio is given by

$$(g_f)_1 / (g_f)_2 = C_1/C_2 .$$

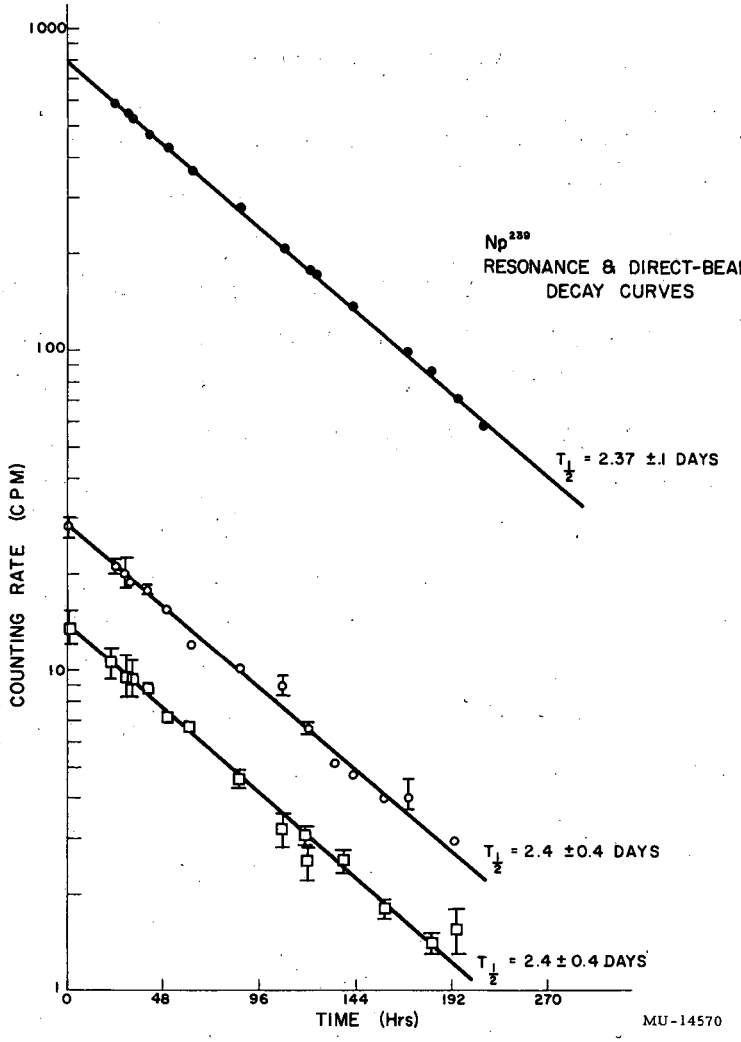

Fig. 27. Results of half-life determination of the sample.

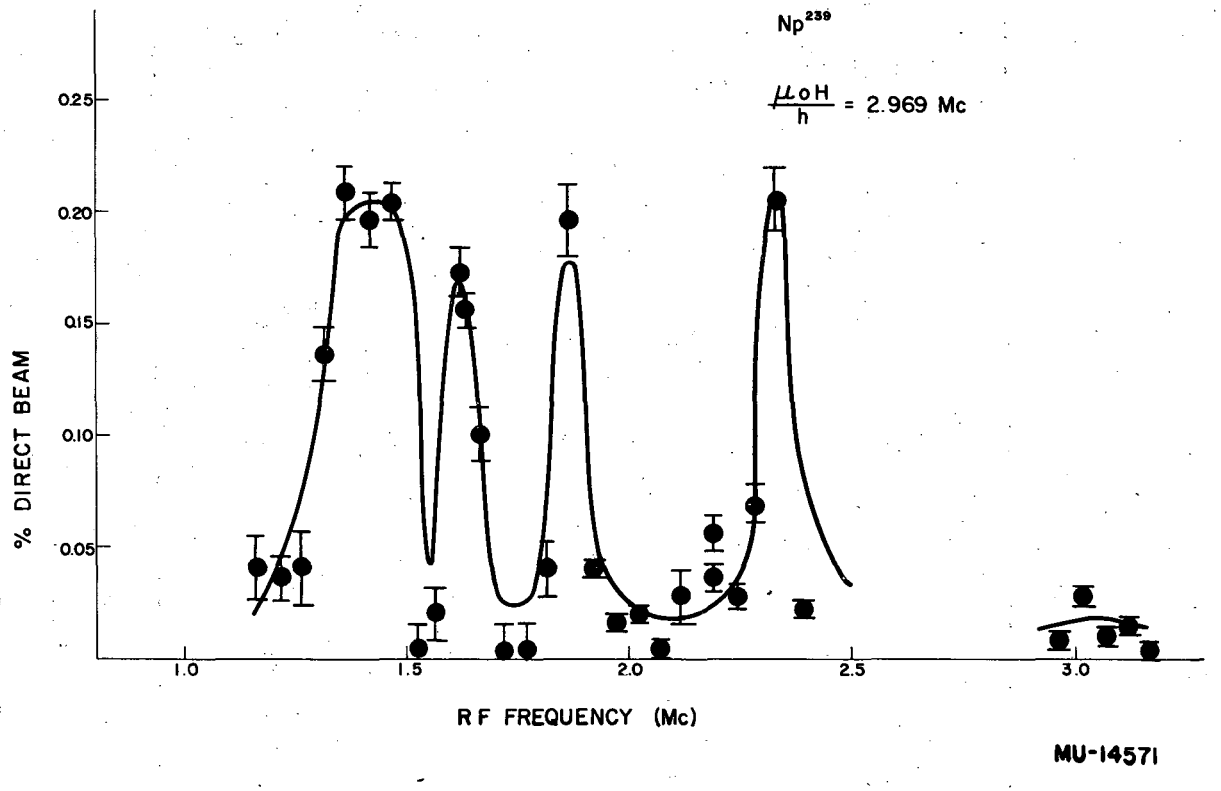

Fig. 28. Results of the resonance search at 2.1 gauss.

Table IV

Summary of data

	Magnetic field $\left(\frac{\mu_0 H}{h}\right)$	Total angular momentum F=8	F=7	F=6	F=5	F=4	F=3
Experimental observations (g_f)	1.443 Mc					0.76 ±0.02	1.04 ±0.02
	1.985 Mc	0.43 ±0.015	0.479 ±0.015	0.534 ±0.015	0.635 ±0.015		
	2.969 Mc	0.451 ±0.010	0.485 ±0.010	0.543 ±0.010	0.624 ±0.010	0.788 ±0.010	
	5.880 Mc	0.451 ±0.005		0.540 ±0.005			
	11.544 Mc	0.449 ±0.003	0.484 ±0.003				
	18.786 Mc		0.4841 ±0.0015				
	27.386 Mc			0.5379 ±0.0010	0.6222 ±0.0010	0.7697 ±0.0010	1.0649 ±0.0010
	35.535 Mc	0.4505 ±0.0008	0.4856 ±0.0008	0.5379 ±0.0008	0.6223 ±0.0008	0.7686 ±0.0008	
Mean experimental value (g_f)		0.4505 ±0.0008	0.4853 ±0.0007	0.5379 ±0.0006	0.6223 ±0.0006	0.7692 ±0.0006	1.065 ±0.0010
Calculated g_f values: J=11/2, I=5/2, g_J = 0.6551, g_I = 0		0.4504	0.4855	0.5381	0.6223	0.7697	1.0645
Observed relative resonance intensities		1	1	0.8	0.5	0.5	0.1
Calculated relative resonance intensities		1	0.8	0.6	0.5	0.3	0.1

The specific procedure was to calculate all possible ratios of the mean experimental g_f values. For a given I, values of C were calculated for many different J's and all possible values of F consistent with the choice of I and J. The ratio of the C values for all F's corresponding to a given I and J were then taken. If they were within one or two mean deviations of any experimentally determined ratio, they were noted.

A fit of this type was attempted for all half-integer values of I from 1/2 through 7/2. In the case I = 1/2, all values of J up to 25/2 were tried with the result that it was impossible to fit any set of the observed ratios which included all six resonances to within two mean deviations. For I = 3/2 and 5/2, half-integer values of J up to 15/2 were tried with no fit found for all the data to within two mean deviations. For I = 7/2 and values of J up to 15/2, no fit could be found to within one mean deviation. For values of I greater than 7/2, the chance of accidentally fitting the data becomes large. The assignment of I = 5/2 rests, however, primarily on the fact that the six individual g_f values can be fitted to well within the experimental error for one value of J(J=11/2), and $g_J = 0.6551 \pm .0006$. Under the assumption of I = 5/2 and J = 11/2, the g_J value was chosen to minimize the root-mean-square error in the experimental g_f values, i.e., to minimize the quantity $\sum_f (g_{f_{exp}} - g_{f_{theor.}})^2$.

Discussion of Results

1. Observed Intensities

The data taken on Np^{239} clearly indicate the existence of transitions in the five states F = 4, 5, 6, 7, 8. The transition in the state F = 3 was never clearly resolved, i.e., the counting rates establishing the peak are close enough to background so that the probability of its not having been observed is perhaps 50%. Failure to clearly observe this peak can be explained on intensity grounds. The hyperfine-structure diagram for the system I = 5/2, J = 11/2 (Fig. 29) indicates the existence in a state F of exactly 2F-5 flop-in transitions. A strictly correct procedure for calculating the relative intensities of the observed transitions would necessitate a procedure of the sort used for curium.

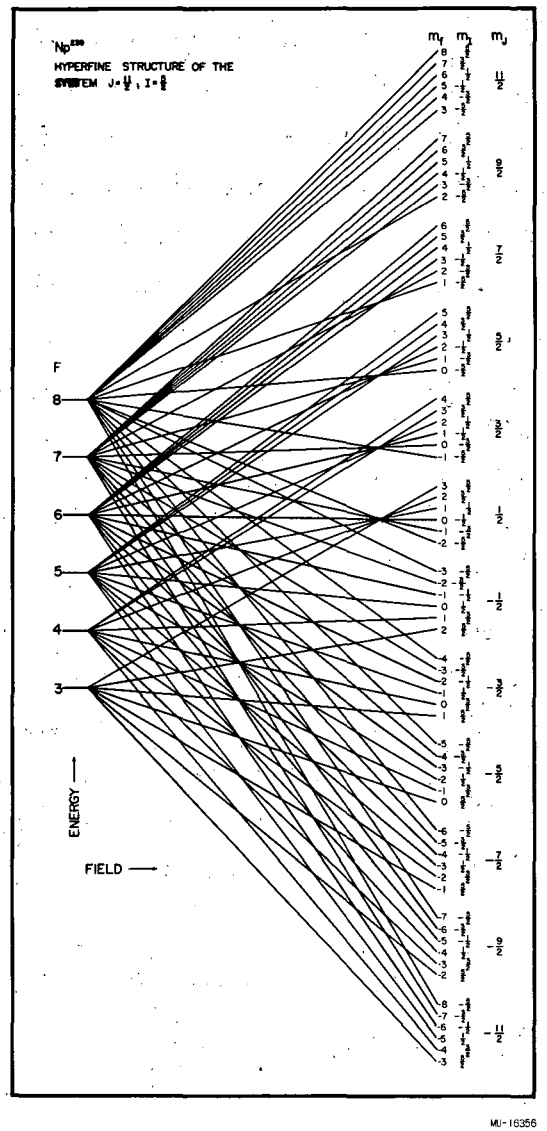

Fig. 29. Energy-level diagram of the system J = 11/2, I = 5/2 in a magnetic field (not to scale).

However, any attempt to make a complete calculation of the transition probabilities would require a machine calculation of a minimum of 300 integrals. Barring a complete calculation of this sort, about the only statement that can be safely made is that with only one transition contributing to the resonance in the state F = 3 it certainly ought to have a much lower intensity than the resonances in the other states. If we make the crude assumption that the resonance in the state F is proportional to the number of flop-in transitions occurring in that state, then the relative intensities will be those shown in Table IV. These are compared with the experimentally observed intensities. It is apparent that the observed intensity in the state F = 3 is of the order of magnitude we expect.

2. Electronic Ground State

The research on neptunium indicates that there exists an electronic level characterized by J = 11/2, $g_J = 0.6551 \pm .0006$, which is very probably the ground state. The existence of such a level is well explained from the assumption of a ground-state configuration $5f^4\ 6d\ 7s^2$ if the same electronic coupling scheme is used which is successful in curium, uranium, and protoactinium. The configuration $5f^4$ couples to the Hund's Rule ground-state term $^5I_4$ with a g value $g_J = 0.559$. The Hund's Rule ground state for 6d is $^2D_{3/2}$ with $g_J = 0.800$. All g values quoted include the effect of the anamolous moment. In pure j-j coupling between the shells, the levels J = 11/2, 9/2, 7/2, and 5/2 are possible. The J = 11/2 level has a value for g of $g_J = 0.6537$ on this idealized scheme. The evidence from the curium research is that the $^2D_{3/2}$ state is slightly perturbed. If, in neptunium, the perturbed state is characterized by J = 3/2, $g_J = 0.8041$, then perfect agreement with experiment is obtained. Measurements on the g_J values of the other J states, perhaps by optical spectroscopy, could establish the validity of this hypothesis.

3. Nuclear Structure

The interpretation of the spin of 5/2 on the Nilsson model has been thoroughly discussed by Hollander.[47] He assigns the odd proton to the state (642+)5/2, although the levels (523-)5/2 and (512-)5/2 are also possible

choices. The reason for the preferred choice is that it is the only one of the three states having positive parity, a condition imposed on the basis of analogy with the Np^{237} ground state. It is worth pointing out that this state assignment is possible only if the deformation parameter has the relatively large value $\eta > +5.8$. The level scheme has not been worked out for large enough values of η to permit statement of an upper limit for η. The Np^{237} quadrupole moment determined by Coulomb excitation is $Q = \pm 1$ barns,[51] and yields a deformation parameter $\eta \approx +5$. A measurement of Q for Np^{239} could establish the deformation in this nucleus.

Using Formula (II.12) for the magnetic field at the nucleus, and the value for $(1/r^3)$ for 5f and 6d electrons in uranium, one can estimate a crude value for the lower limit of the magnetic moment of Np^{239}. From this procedure, and using 20 Mc for the lower limit to the hyperfine structure, one obtains $\mu \geq 0.3$ nm.

NEPTUNIUM-238

Because a low-lying electronic state of neptunium characterized by $J = 11/2$, $g_J = 0.6551$ had been discovered it became desirable to make the relatively routine measurements necessary to determine the spin of Np^{238}. This quantity is of interest for several reasons. Beta- and gamma-ray spectroscopic measurements indicate that the ground-state spin is very probably either 2 or 3.[52] Some Russian work indicates further that if the spin is 2, then the parity can not be even.[53] On the theoretical side, Np^{238} is an odd-odd nuclide, where the states for the last neutron and proton are presumably known from Pu^{239} and Np^{239} respectively. Hence the spin is expected to yield information concerning coupling in the region of strongly deformed nuclei.

Technical Procedure

The prior work on neptunium had already solved the problems of beam chemistry and production. Further, the problem of detection is the same as for Np^{239}, so that the same flow proportional counters could be used.

Material production is by neutron activation of Np^{237}. A mixture of 3 mg of Np^{237} oxide and 10 mg of U^{238} oxide was encapsulated in quartz and bombarded at the Argonne pile, receiving a total integrated flux of 1.0×10^{19} neutrons per cm^2. The U^{238} was present for carrier purposes only. The relative activation cross sections are such that the resultant activity was 95% Np^{238} and 5% Np^{239}.

The near equality of the half lives and beta-ray spectra of Np^{238} and Np^{239} precludes the possibility of identification of the material by these means alone. However, the method of production and the observed integral spin in addition to the measured half life are completely convincing.

Experimental Observations and Discussion

An initial spin search was made in the Zeeman region at a field of 0.70 gauss. Under the assumption that the electronic state being observed has $J = 11/2$, $g_J = 0.6551$, the application of Eq. (II.7) to the resonances indicates a spin of 2. The hyperfine-structure diagram for $I = 2$, $J = 11/2$

is shown in Fig. 30. It is apparent that in the Zeeman region there are five sets of flop-in transitions corresponding to the five F levels. Transitions in the states F = 15/2, 13/2, 11/2, and 9/2 were clearly observed at a field of 13.4 gauss (Fig. 31), where the resolution in g_f is about 0.5% The low intensity of the transition in the state F = 7/2 precluded any definite observation, although a small effect was seen in the frequency region where it was expected. The center frequencies of the observed resonances are given in Table V along with the calculated frequencies for the indicated electronic level and a spin of 2.

On the assumptions I = 2 and J = 11/2, the observed resonances can be used to recalculate the g_J value of the observed electronic state. This yields a value of 0.6553 ± .0010, consistent with the value from the Np^{239} research. Averaging the values, the best value is still 0.6551±.0005.

The observed intensity pattern indicates an anamolously low peak for the state F = 15/2. However, the heights of the remaining peaks, including the one marginally resolved in the state F = 7/2, are explainable by the same assumption used for Np^{239}, namely that the intensity in a given state is proportional to the number of flop-in transitions in the state. The only plausible explanation for F = 15/2 is that the rf current of 30 ma used throughout the experiment was well below optimum. The F = 15/2 state has the lowest g_f value, hence it needs the highest rf current for optimum transition probability.

Nuclear Structure

The problem of coupling in odd-odd nuclei in the region where the deformation is large can be analyzed in terms of the Moszkowski rules, (I.4). For Np^{238}, Ω_P and Ω_N are separately known from Np^{239} and Pu^{239} to be 5/2 and 1/2 respectively. Whether they should couple to two or three depends critically on the state assignment for these particles. The odd neutron seems to fit very well into the state (631-)1/2. However, much less is known about the odd-proton state, and it is possible to assign it to either of the states (642+)5/2 or (523-)5/2. If the proton is assigned to the (642+)5/2 state, then the strong rule applies, and the spin of 2 is in agreement with the stated rules. However, the parity of

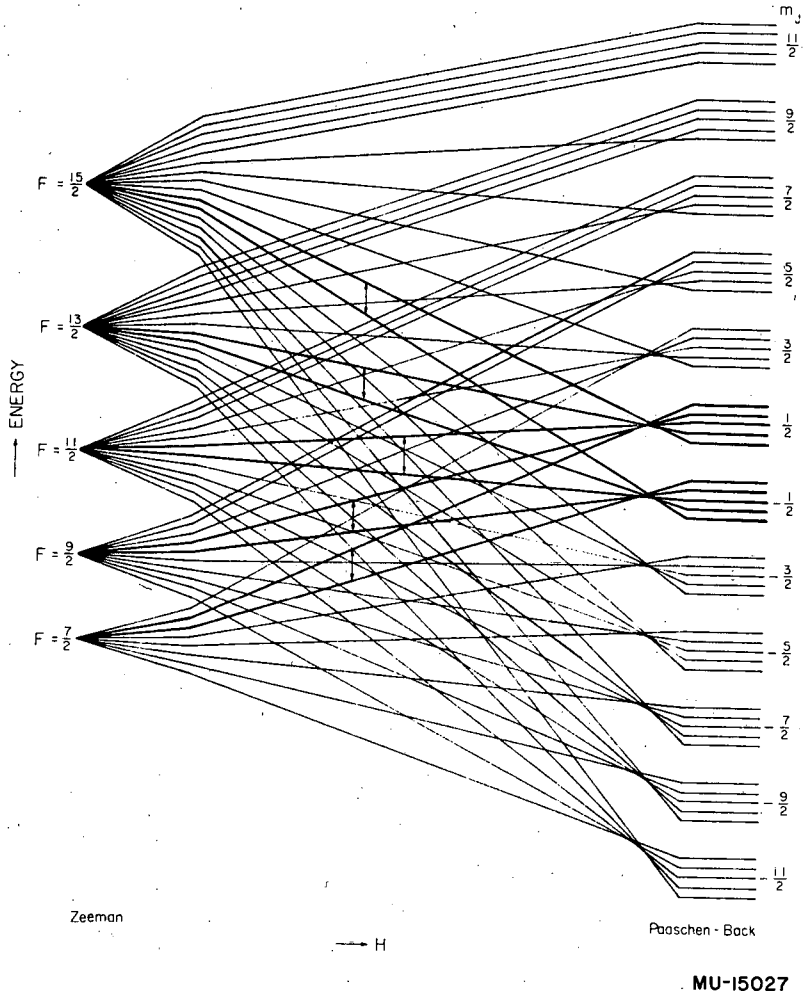

Fig. 30. Energy-level diagram of the system J = 11/2, I = 2 in a magnetic field (not to scale).

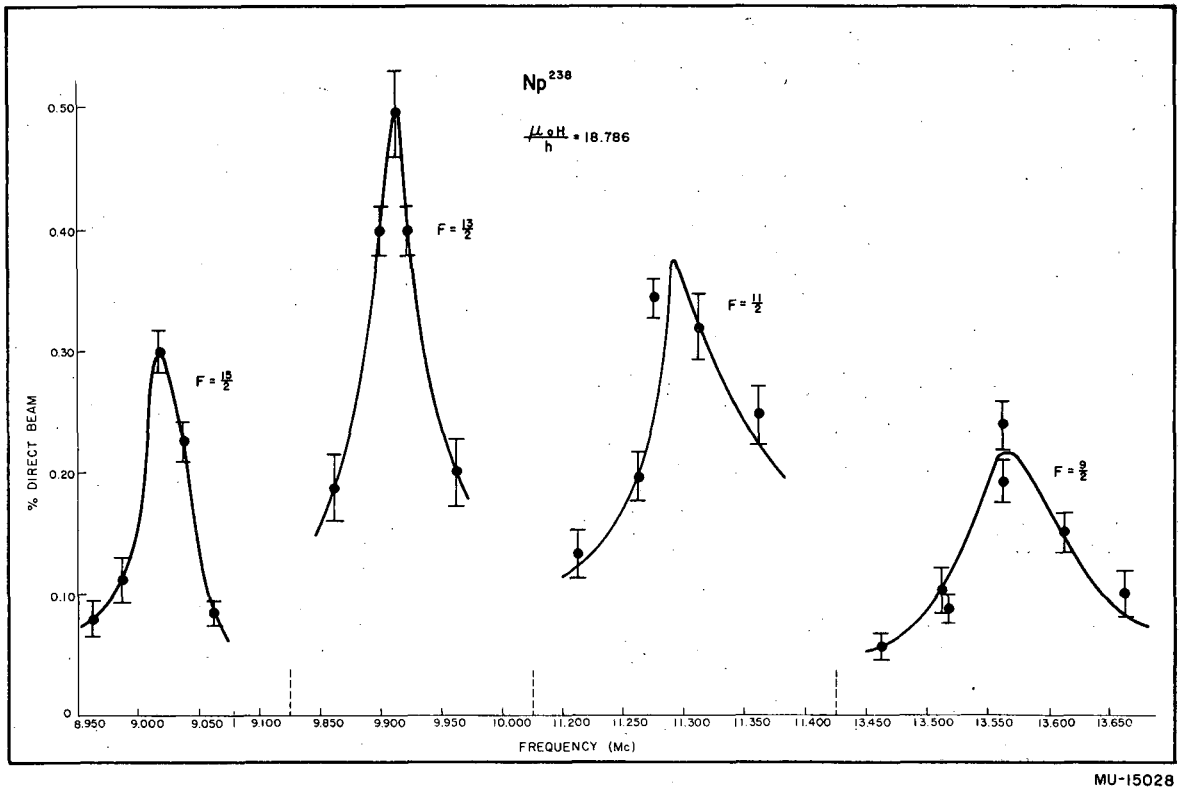

Fig. 31. Observed Np^{238} resonances at 13.4 gauss.

Table V

Summary of Observations					
	State				
	F = 15/2	F = 13/2	F = 11/2	F = 9/2	F = 7/2
Observed frequency(Mc)	9.020± 0.025	9.912± 0.025	11.290± 0.035	13.562± 0.025	17.790± 0.050
Predicted frequency(Mc)	9.025	9.908	11.274	13.550	17.776

the system is positive and in disagreement with the Russian beta-decay work. On the other hand, the assignment of (523-)5/2 as the odd-proton state gives negative parity, but is in disagreement with the coupling rules. Clearly, more experimental information on the parities of the ground states of Np^{238} and Np^{239} is needed to settle these questions.

A lower limit to the magnetic moment of this isotope can be inferred from the measurements if one uses the same value for the magnetic field at the nucleus as is obtained in Np^{239}. This yields $\mu \geq 0.3$ nm.

ACKNOWLEDGMENTS

It has been a source of great knowledge, inspiration, and pleasure to have been a graduate student of Professor William Nierenberg. I have always found his many ideas and constant enthusiasm extremely stimulating.

I owe a debt of appreciation to Dr. J. C. Hubbs for relieving the burden of my woeful ignorance concerning experimental technique. The many hours spent together in the laboratory have been a source of much enlightening information and discussion.

My association with other graduate students in the group has been extremely pleasant. Joe Winocur and Amado Cabezas have been very generous with their aid in many of the runs. To Dr. John Worcester, who was constantly helpful during the difficult early months of my experimental education, I am especially grateful.

I have had many interesting and helpful discussions with Dr. Edgar Lipworth and Dr. Howard Shugart. Dr. James Wallman and other members of the chemistry group have given much helpful assistance with the chemistry problems arising in this work.

Finally, I am delighted with this opportunity to thank my mother for all the support and encourgement she has given me during by college career.

This work was done under the auspices of the U.S. Atomic Energy Commission.

REFERENCES

1. Hubbs, Nierenberg, Marrus, and Worcester, Phys. Rev. 109, 390 (1958);
   J.C. Hubbs and R. Marrus, Phys. Rev. 110, 287 (1958);
   Albridge, Hubbs, and Marrus, Phys. Rev. 111, 1137 (1958);
   Hubbs, Marrus, and Winocur, Phys. Rev. (to be published).
2. For a discussion of this point, see Mayer and Jensen, Elementary Theory of Nuclear Shell Structure (John Wiley and Sons, Inc. New York, 1955), Chap. 8.
3. J. Rainwater, Phys. Rev. 79, 432 (1950).
4. A. Bohr, Phys. Rev. 81, 134 (1951), and Kgl. Danske, Videnskab. Selskab. Mat.-fys. Medd. 26, No. 14 (1952);
   A. Bohr and B.R. Mottelson, Kgl. Danske Videnskab. Selskab. Mat.-fys. Medd. 27, No. 16 (1953).
5. D.L. Hill and J.A. Wheeler, Phys. Rev. 89, 1102 (1953);
   K.W. Ford, Phys. Rev. 90, 1929 (1953);
   Wilets, Hill, and Ford, Phys. Rev. 90, 1388 (1953).
6. A. Bohr and B.R. Mottelson, Kgl. Danske Matt.-fys. Medd. (Royal Danish Acad.), 27, No. 16 14 (1953).
7. S.G. Nilsson, Kgl. Danske Videnskab. Selskab Matt.-fys. Medd. 29, No. 16 (1955).
8. C.J. Gallagher, Jr. and S.A. Moszkowski, Phys. Rev. 111, 1282 (1958).
9. A. Bohr and B.R. Mottelson, Beta and Gamma Ray Spectroscopy, K. Siegbahn, Ed., (North Holland Publishing Company, Amsterdam 1955). Chap. 17.
10. Y. Suguira and H.C. Urey, Kgl. Danske Videnskab. Selskab, Matt.-fys. Medd. 7, No. 13, 3 (1926);
    N. Bohr, Nature 112, 29 (1923);
    M.G. Mayer, Phys. Rev. 60, 184 (1941);
    T.S. Wu and S. Goudsmit, Phys. Rev. 43, 496 (1933);
    V. Karapetoff, J. Franklin Inst. 210, 609 (1930);
    G.E. Villar, J. Chem. Educ. 19, 329 (1942).

11. Earl K. Hyde and G. T. Seaborg, Handbuch der Physik, Volume 39.
12. General treatments of this subject are given by the following authors: C. Schwartz, Phys. Rev. 97, 380 (1955); H.B.G. Casimir, On the Interaction Between Atomic Nuclei and Electrons (Teyler's Tweede Genootschap, Haarlem, 1936).
13. N.F. Ramsey, Molecular Beams (Oxford University Press, London, 1956), Chaps. 3, 9.
14. C. Schwartz, Phys. Rev. 97, 380 (1955).
15. W.A. Nierenberg (Univ. of California), private communication.
16. G. Breit and I.I. Rabi, Phys. Rev. 38, 2082 (1931).
17. E. Fermi, Physik 60, 320 (1930).
18. F. Low and E.E. Salpeter, Phys. Rev. 83, 478 (1951), 77, 361 (1950).
19. G. Breit, Nature 122, 649 (1928); G. Breit, Phys. Rev. 35, 1447 (1930); G. Breit and L. Wills, Phys. Rev. 44, 470 (1933); G. Breit and G.E. Brown, Phys. Rev. 73, 1278, (1948); Breit, Brown, and Arfken, Phys. Rev. 76, 1299 (1949); H. Margenau, Phys. Rev. 57, 383 (1940).
20. J. Schwinger, Phys. Rev. 73, 416 (1948), 76, 790 (1949).
21. A.G. Prodell and P. Kusch, Phys. Rev. 79, 1009 (1950), 88, 184 (1952).
22. S. Goudsmit, Phys. Rev. 43, 636 (1933); E. Fermi and E. Segrè, Rendi. Accad. sci.fis. mat. (Soc. reale Napoli) 4, 131 (1931); Z. Physik 82, 729 (1933).
23. N.F. Ramsey, Nuclear Moments (John Wiley and Sons, Inc., New York, 1953).
24. J.R. Zacharias, Phys. Rev. 61, 270 (1942).
25. Rabi, Zacharias, Millman, and Kusch, Phys. Rev. 53, 318 (1938).
26. E. Majorana, Nuovo cimento 9, 43 (1932).
27. Robert J. Sunderland, Nuclear Spins of Rubidium-82, Rubidium-83, and Rubidium-84 (thesis), University of California, 1957 (unpublished).
28. P. Kusch and H. Taub, Phys. Rev. 75, 1477 (1945).
29. Gilbert O. Brink, Nuclear Spins of Thallium-197, Thallium-198m, Thallium-199, and Thallium-204 (thesis) UCRL-3642, June 1957 (unpublished).

30. Brink, Hubbs, Nierenberg, and Worcester, Phys. Rev. 107, 189 (1957).
31. H.N. Russell, J. Opt. Soc. Am. 40, 550 (1950).
32. Van den Berg, Klinkenberg, and Regnaut, Physica 20, 461 (1954).
33. Bleaney, Llewellyn, Pryce, and Hall, Phil. Mag. 45, 773 (1954).
34. Stanley Cohen, Lawrence Radiation Laboratory, private communication.
35. H.B.G. Casimir, On the Interaction Between Atomic Nuclei and Electrons (Teyler's Tweede Genootschap, Haarlem, 1936).
36. W.E. Lamb, Jr., Phys. Rev. 60, 817 (1941).
37. John G. Conway, Lawrence Radiation Laboratory private communication.
38. Hollander, Smith, and Mihelich, Phys. Rev. 102, 740 (1956); J.M. Hollander, Lawrence Radiation Laboratory, private communication.
39. I. Perlman and F. Asaro, Ann. Rev. Nuclear Sci. 4, 157 (1954); Newton, Rose,and Milsted, Phil. Mag. (to be published)
40. J.G. Conway and R.D. McLaughlin, Phys. Rev. 94, 498 (1954).
41. Abraham, C. Jeffries, Kedzie, and Wallmann, Phys. Rev. 106, 1357 (1957).
42. Abraham, Jeffries, Kedzie, and Wallmann, Phys. Rev. (to be published).
43. Asaro, Stephens, Gibson, Glass, and Perlman, Phys. Rev. 103, 1541 (1955); F. Asaro and I. Perlman, Phys. Rev. 93, 1423 (1954).
44. J.M. Hollander, Phys. Rev. 105, 1518 (1957).
45. M. Fred and F.S. Tompkins, Phys. Rev. 89, 318 (1953); J.G. Conway and R.D. McLaughlin, Phys. Rev. 94, 498 (1954).
46. J.E. Mack, Revs. Modern Phys. 22, 64 (1950).
47. Jack M. Hollander, Lawrence Radiation Laboratory, private communication.
48. Neutron Cross Sections, compiled by D.J. Hughes and J.A. Harvey, BNL-325, (July 1955.)
49. H. Slatis, Nature 160, 579 (1947); Arkiv. Mat., Astron. Fysik 36A, No. 21, (1949); H.W. Fulbright, NNES-PPR 14B, 1011 (1949).
50. L. Wish, Nucleonics 14, No. 5, 102 (1956).
51. J.O. Newton, Nuclear Physics (to be published).

52. Rasmussen, Slatis, and Passell, Phys. Rev. 99, 42 (1955); Rasmussen, Stevens, Strominger, and Astron, Phys. Rev. 99, 47 (1955); R.G. Albridge and J.M. Hollander, UCRL-8034, Nov. 1957 (unpublished).

53. S.A. Baranov and K.N. Shlyagin, Atomnaya Energ. 1, 52 (1956) (translation: J. Nuclear Energy 3, 132 1956).

This report was prepared as an account of Government sponsored work. Neither the United States, nor the Commission, nor any person acting on behalf of the Commission:

A. Makes any warranty or representation, express or implied, with respect to the accuracy, completeness, or usefulness of the information contained in this report, or that the use of any information, apparatus, method, or process disclosed in this report may not infringe privately owned rights; or

B. Assumes any liabilities with respect to the use of, or for damages resulting from the use of any information, apparatus, method, or process disclosed in this report.

As used in the above, "person acting on behalf of the Commission" includes any employee or contractor of the Commission to the extent that such employee or contractor prepares, handles or distributes, or provides access to, any information pursuant to his employment or contract with the Commission.